A sub-percent Determination of the Nucleon Axial Coupling from Lattice QCD

Zack B. Hall II
NSF MPS - ASCEND Postdoctoral Fellow
Nuclear Science Division
Lawrence Berkeley National Laboratory

INT WORKSHOP: TESTING THE STANDARD MODEL IN CHARGED-WEAK DECAYS
JANUARY 12-16, 2026

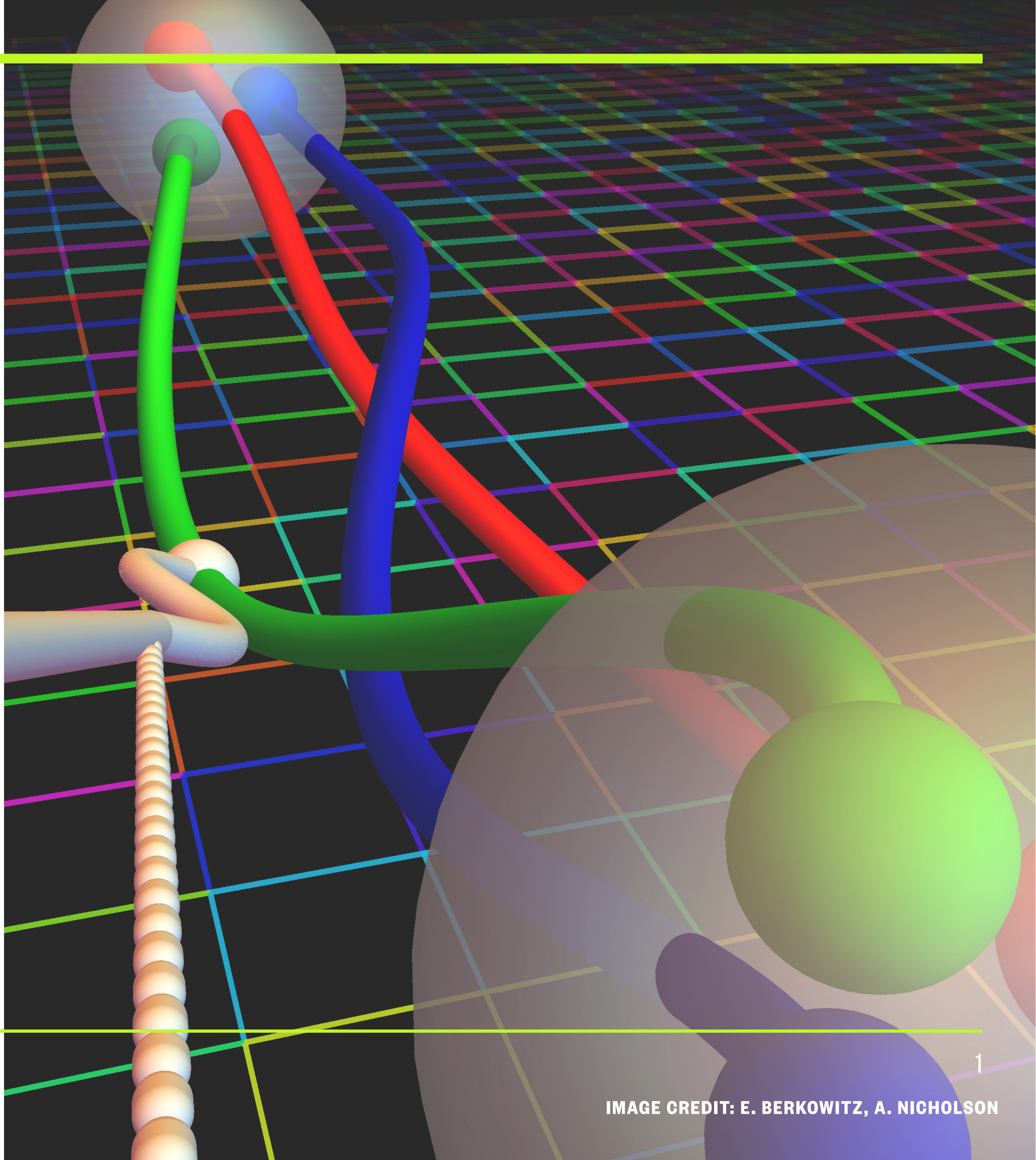

IMAGE CREDIT: E. BERKOWITZ, A. NICHOLSON

Low-Energy Precision Physics

- The transition matrix element for Neutron Beta Decay can be expressed as:

$$M(n \to p e^- \bar{\nu}_e) \sim V_{ud}\, \underbrace{\langle p(p') \,|\, W_\mu \,|\, n(p) \rangle}\, L_\mu$$

$$W_\mu = V_\mu - A_\mu$$

In the zero-momentum limit

$$V_\mu = \bar{u}\gamma_\mu d \longrightarrow g_V \sim \langle p \,|\, \bar{u}\gamma_\mu d \,|\, n \rangle$$

$$A_\mu = \bar{u}\gamma_\mu\gamma_5 d \longrightarrow g_A \sim \langle p \,|\, \bar{u}\gamma_\mu\gamma_5 d \,|\, n \rangle$$

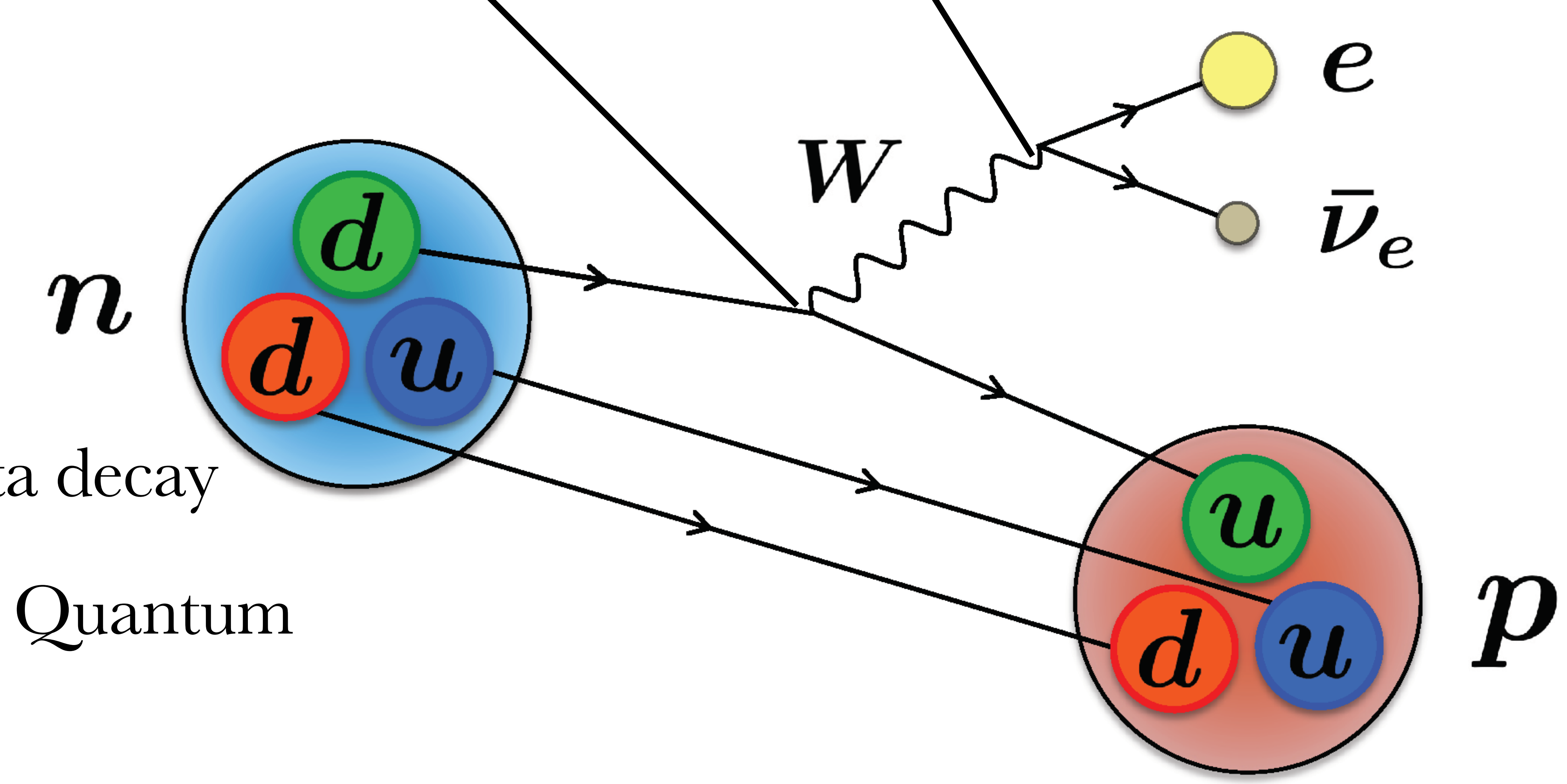

- g_A and g_V can be experimentally measured through Neutron beta decay
- Can be theoretically determined nonperturbatively with Lattice Quantum Chromodynamics.

Image credit: Universe 2023, 9(10), 449

Low-Energy Precision Physics

- Neutron Decay Rate → V_{ud}:

$$|V_{\mathrm{ud}}|^2 = \frac{5099.3(2.7)\mathrm{s}}{\tau_n(1+3\lambda^2)(1+\delta_{\mathrm{RC}})} \qquad \lambda = g_A/g_V$$

  - Neutron beta decay gives τ_n.
  - UCN beta-asymmetry gives λ, which has QED radiative corrections from δ_{RC}.

$$V_{ud}^{n,\mathrm{PDG}} = 0.97441(3)_f(13)_{\Delta_V^R}(82)_\lambda(28)_{\tau_n}[88]_{\mathrm{total}}$$

$$V_{ud}^{0^+\to 0^+} = 0.97367(11)_{\mathrm{exp}}(13)_{\Delta_V^R}(27)_{\mathrm{NS}}[32]_{\mathrm{total}}$$

Phys. Rev. Lett. 120, 202002 [1802.01804]

Low-Energy Precision Physics

- Neutron Decay Rate → V_{ud}:

$$|V_{\rm ud}|^2 = \frac{5099.3(2.7)\mathrm{s}}{\tau_n(1+3\lambda^2)(1+\delta_{\rm RC})}$$

  - Neutron beta decay gives τ_n.
  - UCN beta-asymmetry gives λ, which has QED radiative corrections from $\delta_{\rm RC}$.

$$V_{ud}^{n,\mathrm{PDG}} = 0.97441(3)_f(13)_{\Delta_V^R}(82)_\lambda(28)_{\tau_n}[88]_{\rm total}$$

  - Neutron lifetime puzzle could be resolved with updated Beam-type measurements.

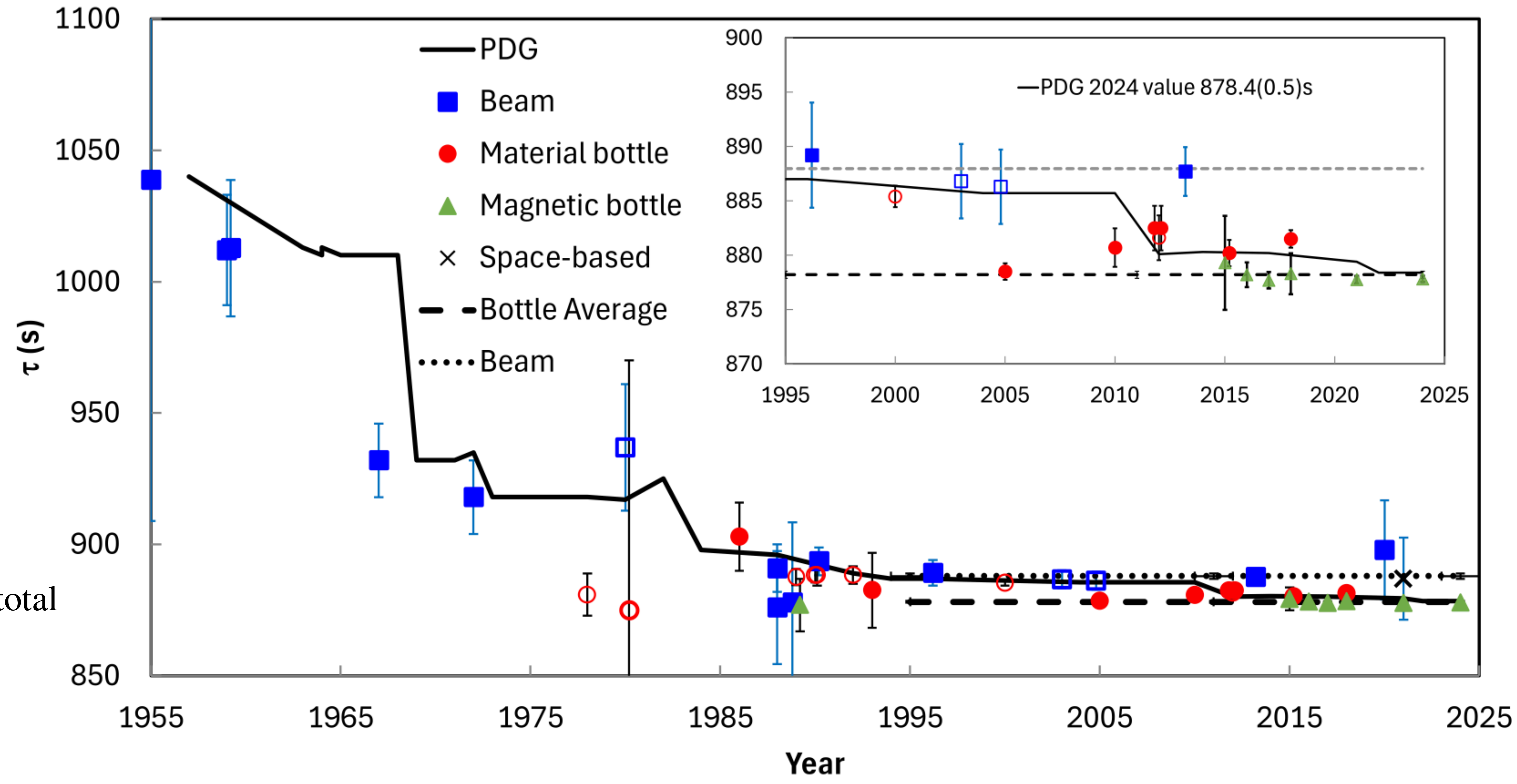

Phys. Rev. Lett. 120, 202002 [1802.01804]

Phys. Rev. C **111**, 045501 (2025) [2409.05560]

Low-Energy Precision Physics

- Neutron Decay Rate → V_{ud}:

$$|V_{\mathrm{ud}}|^2 = \frac{5099.3(2.7)\mathrm{s}}{\tau_n(1+3\lambda^2)(1+\delta_{\mathrm{RC}})} \qquad \lambda = g_A/g_V$$

  - Neutron beta decay gives τ_n.
  - UCN beta-asymmetry gives λ, which has QED radiative corrections from δ_{RC}.

$$V_{ud}^{n,\mathrm{PDG}} = 0.97441(3)_f(13)_{\Delta_V^R}(82)_\lambda(28)_{\tau_n}[88]_{\mathrm{total}}$$

  - Neutron lifetime puzzle could be resolved soon with updated Beam-type measurements.
  - λ distinguishable ~0.2% level with LQCD

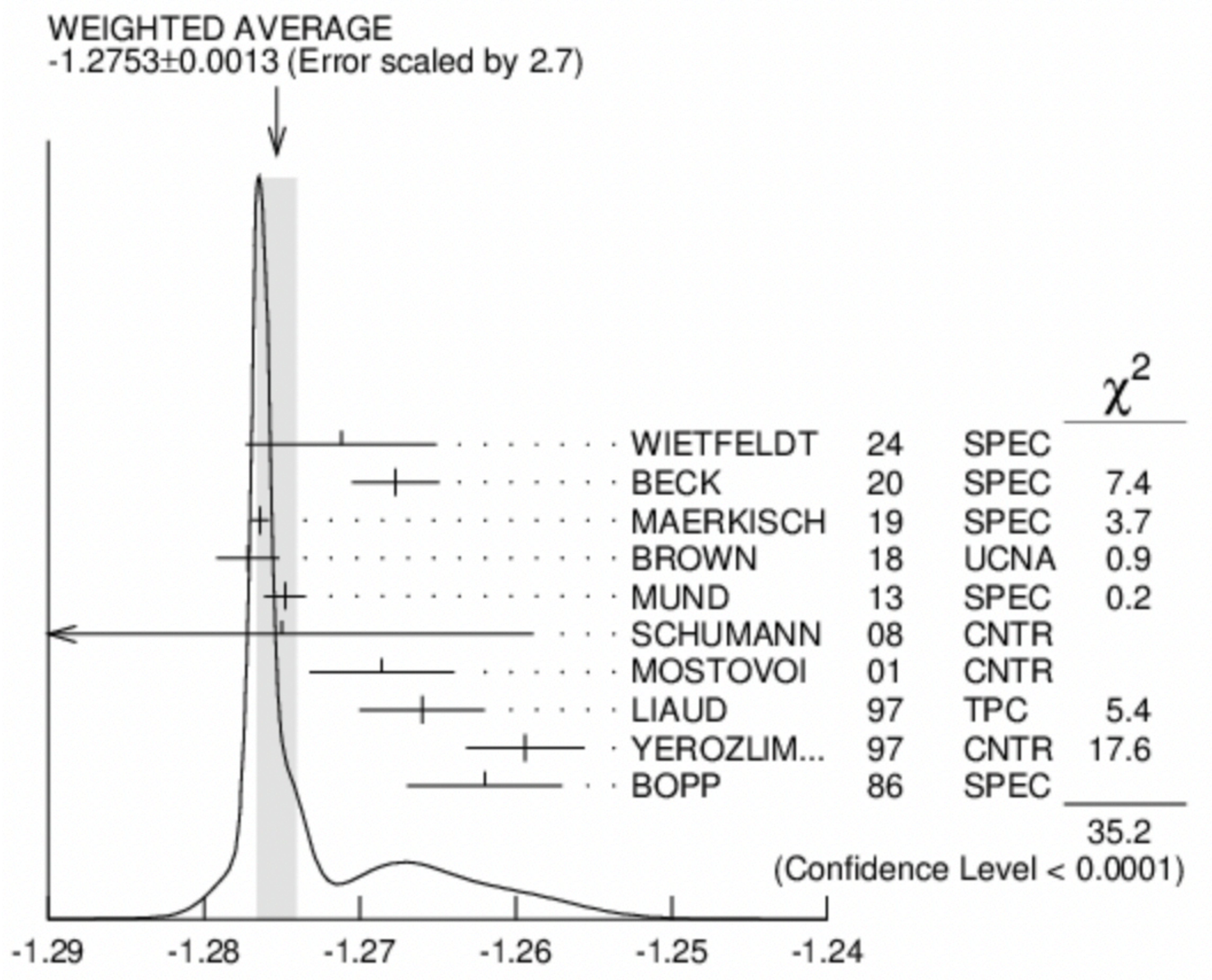

Low-Energy Precision Physics

- Neutron Decay Rate → V_{ud}:

$$|V_{\mathrm{ud}}|^2 = \frac{5099.3(2.7)\mathrm{s}}{\tau_n(1+3\lambda^2)(1+\delta_{\mathrm{RC}})} \qquad \lambda = g_A/g_V$$

  - Neutron beta decay gives τ_n.
  - UCN beta-asymmetry gives λ, which has QED radiative corrections from δ_{RC}.

$$V_{ud}^{n,\mathrm{PDG}} = 0.97441(3)_f(13)_{\Delta_V^R}(82)_\lambda(28)_{\tau_n}[88]_{\mathrm{total}}$$

  - Neutron lifetime puzzle could be resolved soon with updated Beam-type measurements.
  - λ distinguishable ~0.2% level with LQCD

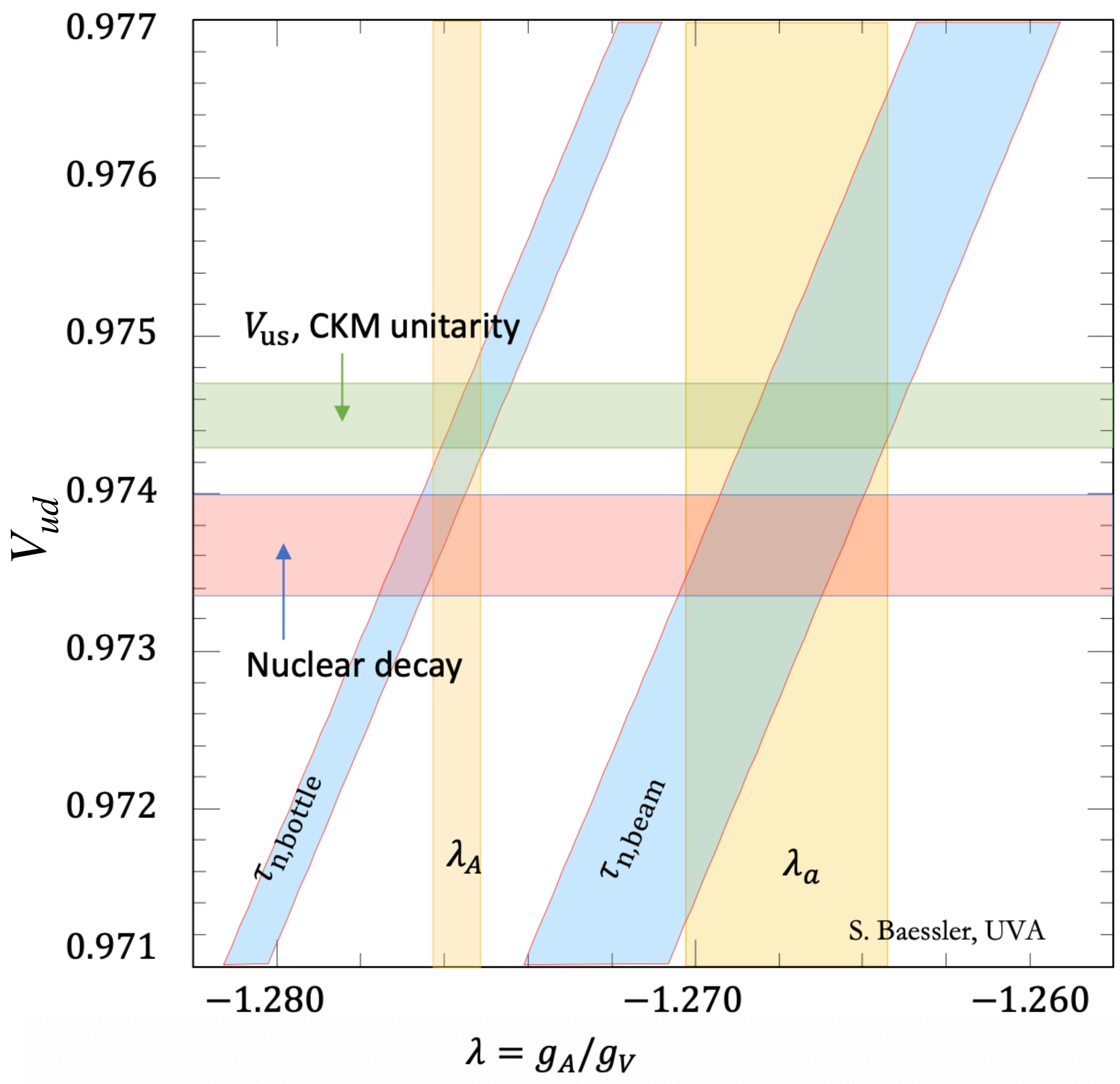

Low-Energy Precision Physics

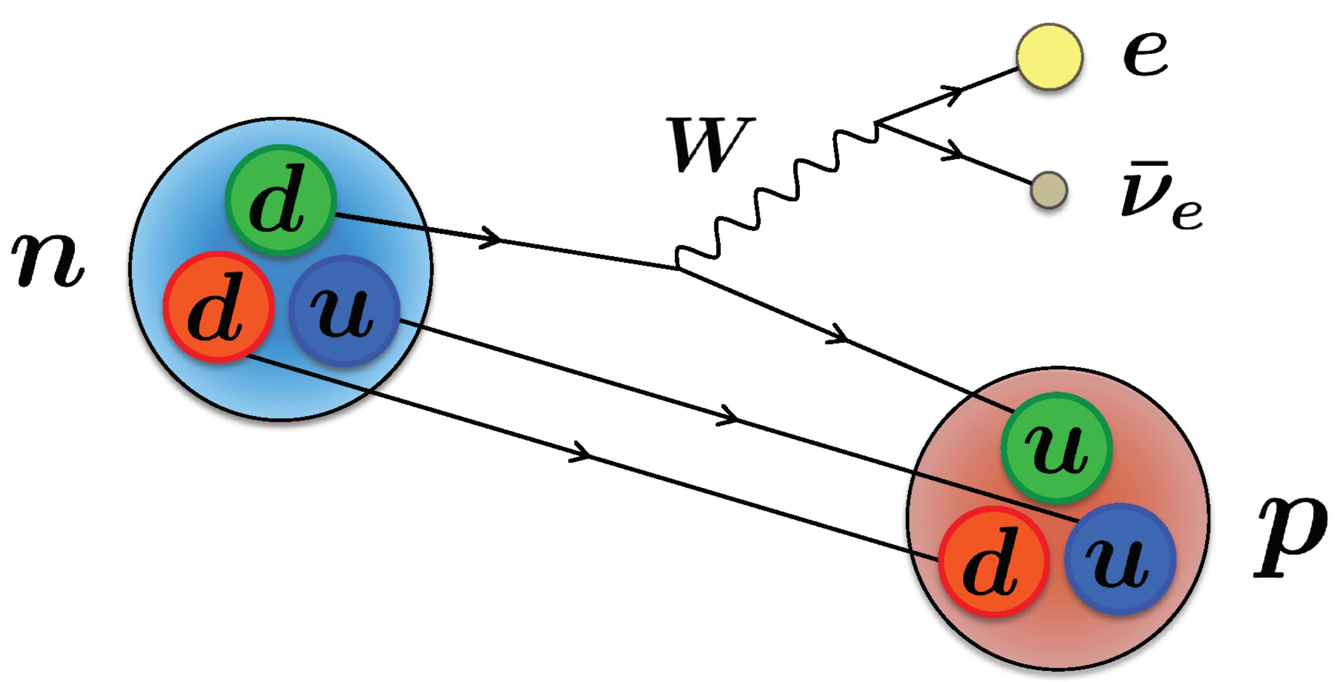

- We can calculate the purely strong contribution of neutron decay through g_A:

$$g_A^{\text{iso}} \sim \langle p \,|\, \bar{u}\gamma^3\gamma^5 d \,|\, n\rangle = \langle p \,|\, \bar{u}\gamma^3\gamma^5 u - \bar{d}\gamma^3\gamma^5 d \,|\, n\rangle$$

- Began as a benchmark quantity… However, challenged by systematic effects:
  - Excited State Contamination
  - Difficulty controlling the chiral-continuum-IV extrapolations

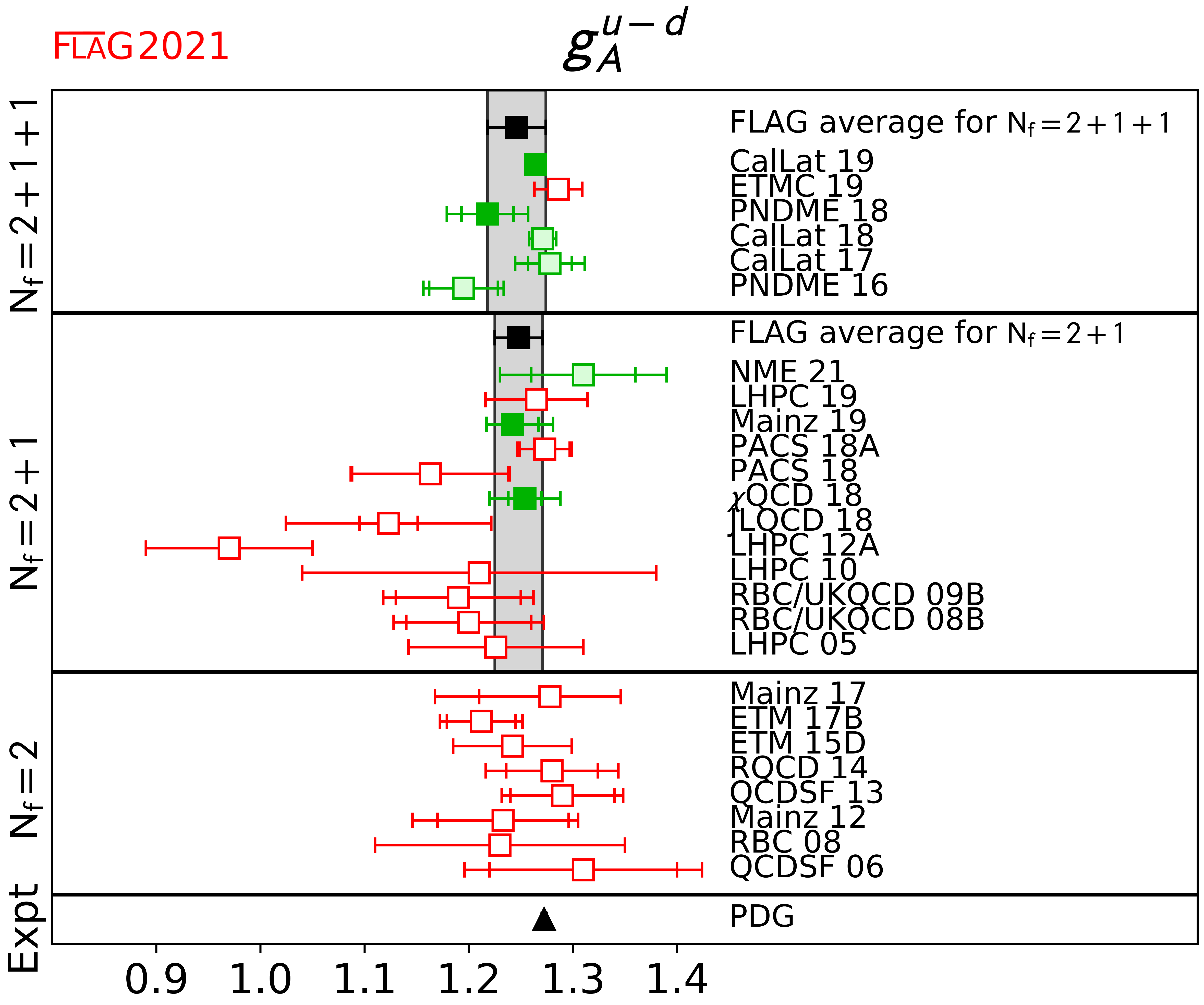

FLAG2024: 2411.04268

Image credit: Universe 2023, 9(10), 449

Low-Energy Precision Physics

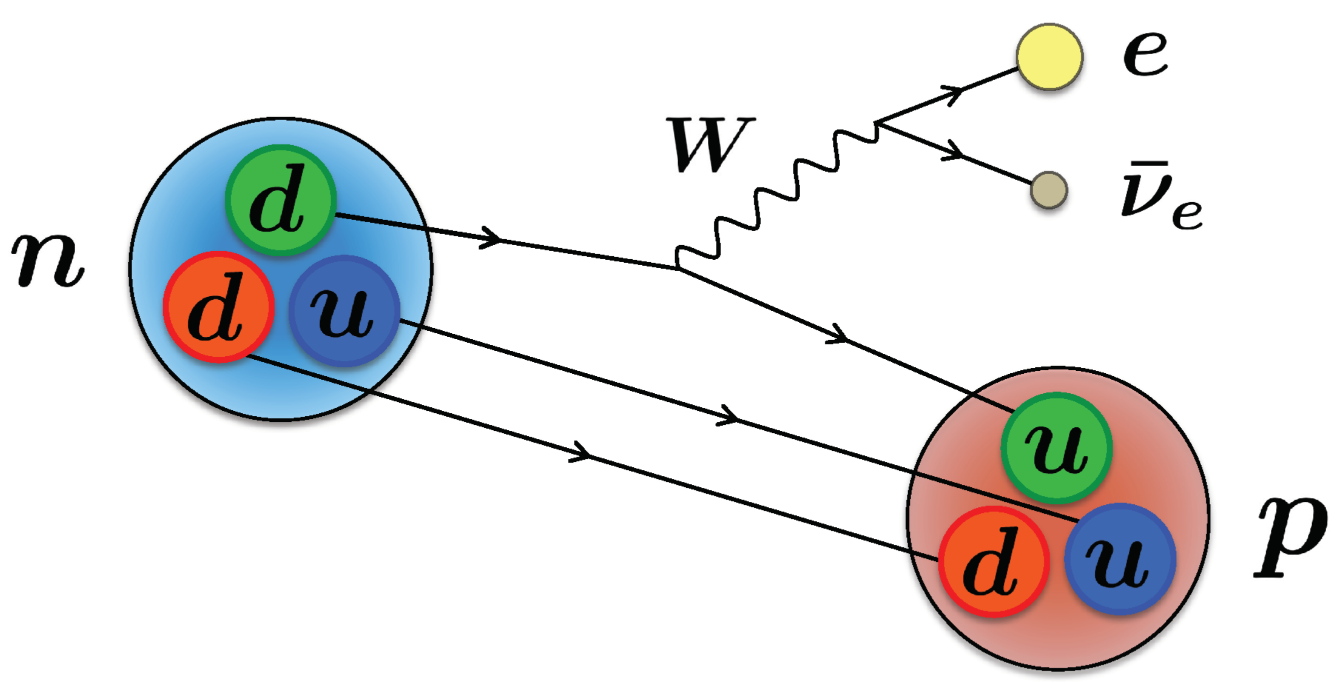

- We can calculate the purely strong contribution of neutron decay through g_A:

$$g_A^{\text{iso}} \sim \langle p \,|\, \bar{u}\gamma^3\gamma^5 d \,|\, n \rangle = \langle p \,|\, \bar{u}\gamma^3\gamma^5 u - \bar{d}\gamma^3\gamma^5 d \,|\, n \rangle$$

- Began as a benchmark quantity -> precision observable.
- As the statistical precision increases, we as a community must continue to scrutinize our methods for characterizing systematic effects.

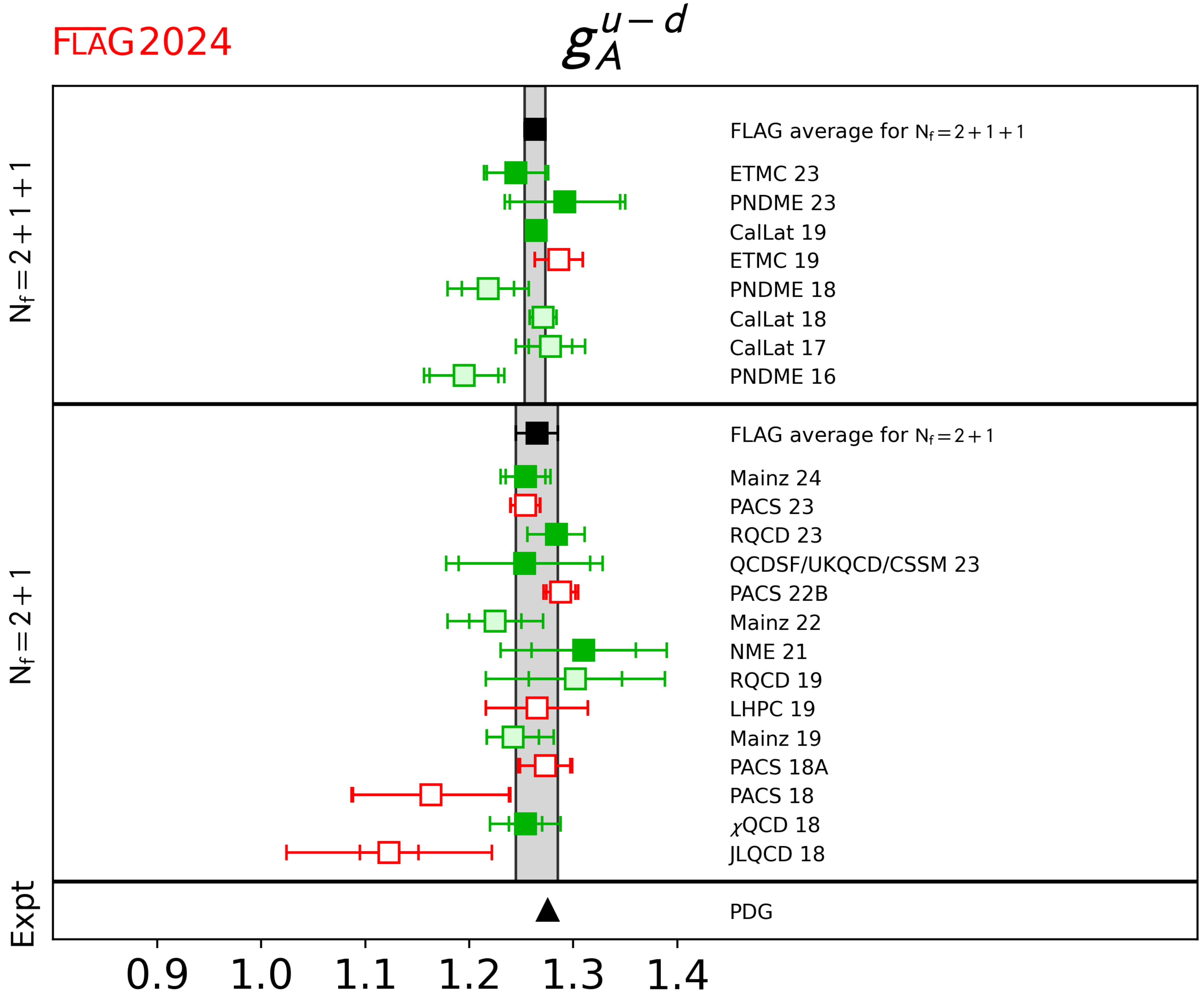

FLAG2024: 2411.04268

Image credit: Universe 2023, 9(10), 449

CalLat and friends Update to g_A

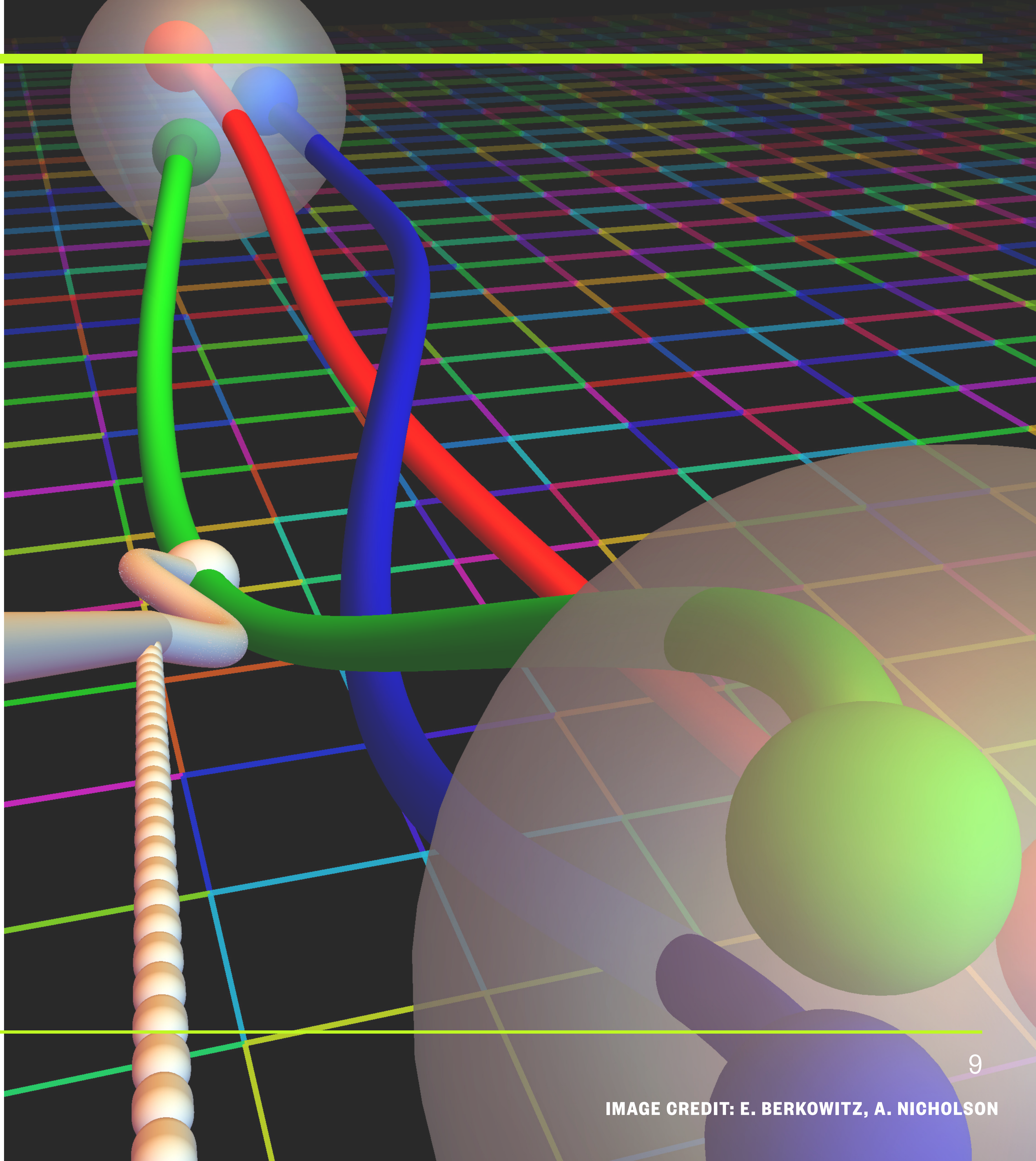

This work: arXiv: 2503.09891 [hep-lat]

IMAGE CREDIT: E. BERKOWITZ, A. NICHOLSON

Correlation Functions

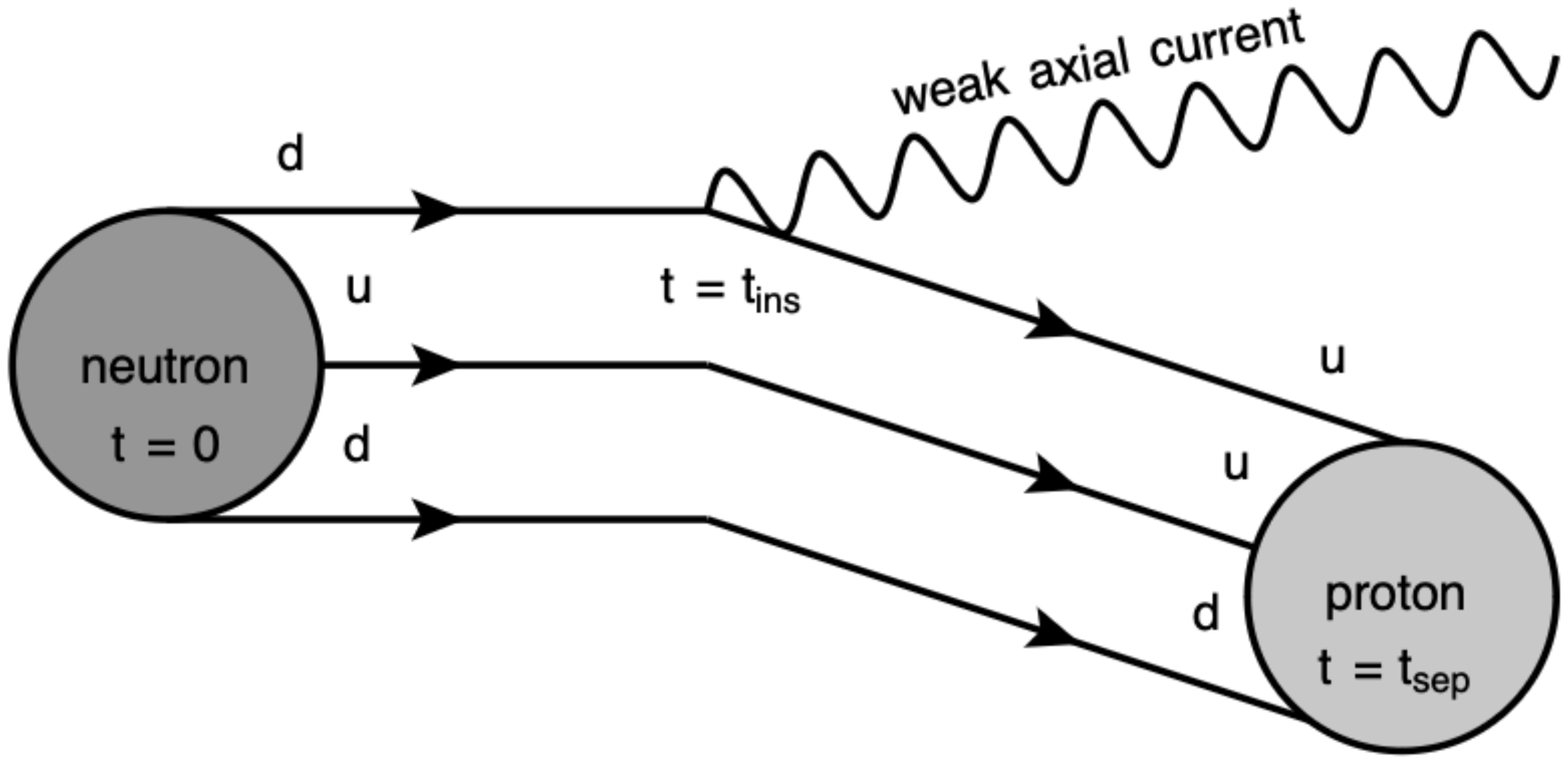

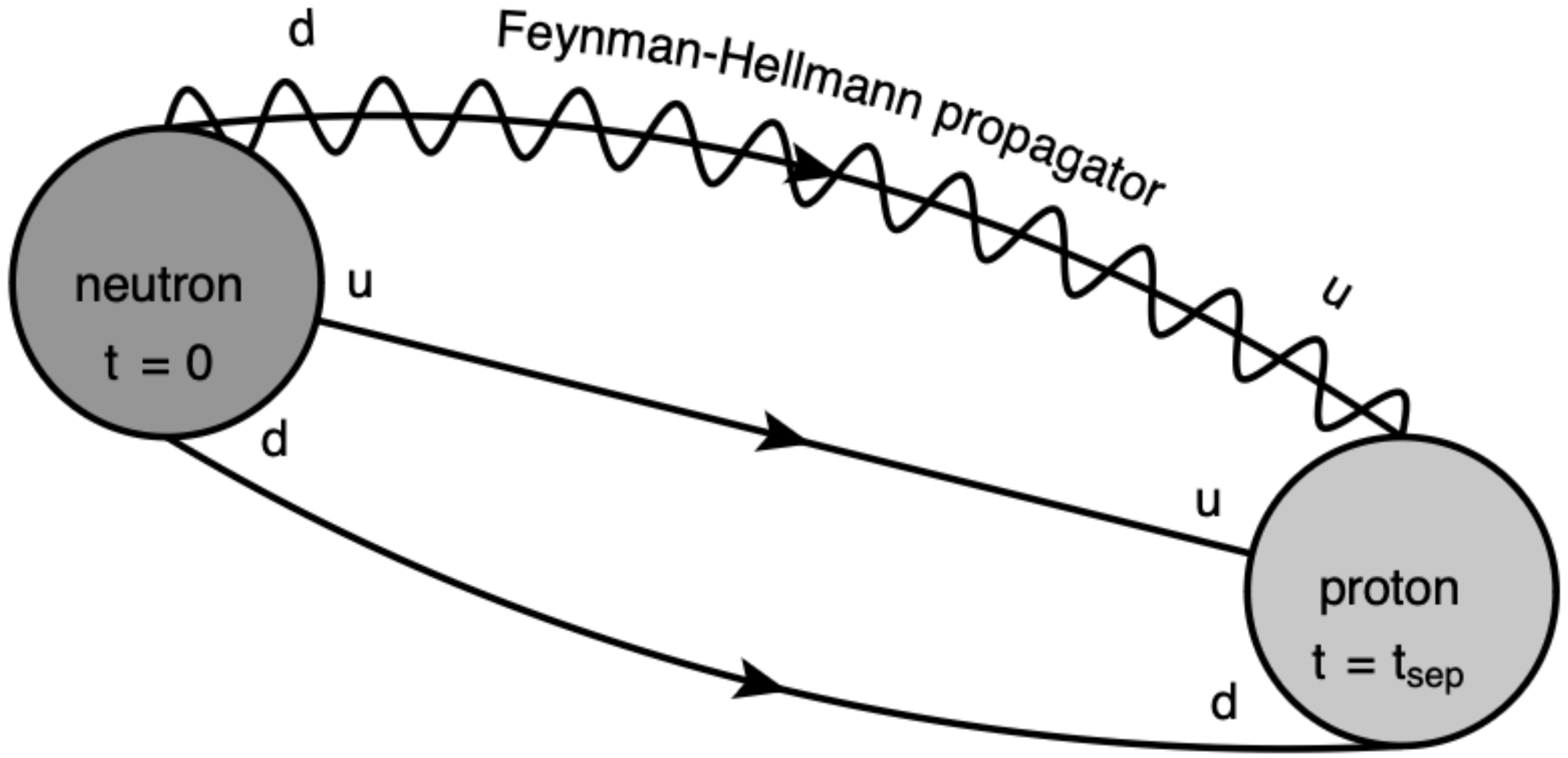

$$-\partial_\lambda C_\lambda(t)\,|_{\lambda=0} = \sum_{n=0}^{N} (t-1)\left[\,|A_n|^2\, g^\Gamma_{nn} - d_n\right] e^{-E_n t} + 2\sum_{n<m} A_n A_m^\dagger\, g^\Gamma_{nm}\, e^{(-E_n+\Delta_{mn}/2)t}\, \frac{\sinh\left[\Delta_{mn}(t+1)/2\right]}{\sinh\left(\Delta_{mn}/2\right)}$$

$$C_{3\mathrm{pt}}(t,\tau) = \sum_{n} |A_n|^2\, g^\Gamma_{nn}\, e^{-E_n t} + 2\sum_{n<m} A_n A_m^\dagger\, g^\Gamma_{nm}\, e^{(-E_n+\Delta_{nm}/2)t}\, \cosh\left[\Delta_{mn}\left(\tau - \frac{t}{2}\right)\right]$$

Image credit: Nature 558, 91–94 (2018)

Correlation Functions

- Sum over τ vs multiple insertion times

$$-\partial_\lambda C_\lambda(t)\,|_{\lambda=0} = \sum_{n=0}^{N}(t-1)\left[\,|A_n|^2 g^\Gamma_{nn} - d_n\right] e^{-E_n t} + 2\sum_{n<m} A_n A^\dagger_m\, g^\Gamma_{nm}\, e^{(-E_n+\Delta_{mn}/2)t}\,\frac{\sinh\left[\Delta_{mn}(t+1)/2\right]}{\sinh\left(\Delta_{mn}/2\right)}$$

$$C_{3\text{pt}}(t,\tau) = \sum_n |A_n|^2 g^\Gamma_{nn}\, e^{-E_n t} + 2\sum_{n<m} A_n A^\dagger_m\, g^\Gamma_{nm}\, e^{(-E_n+\Delta_{nm}/2)t}\,\cosh\left[\Delta_{mn}\left(\tau-\frac{t}{2}\right)\right]$$

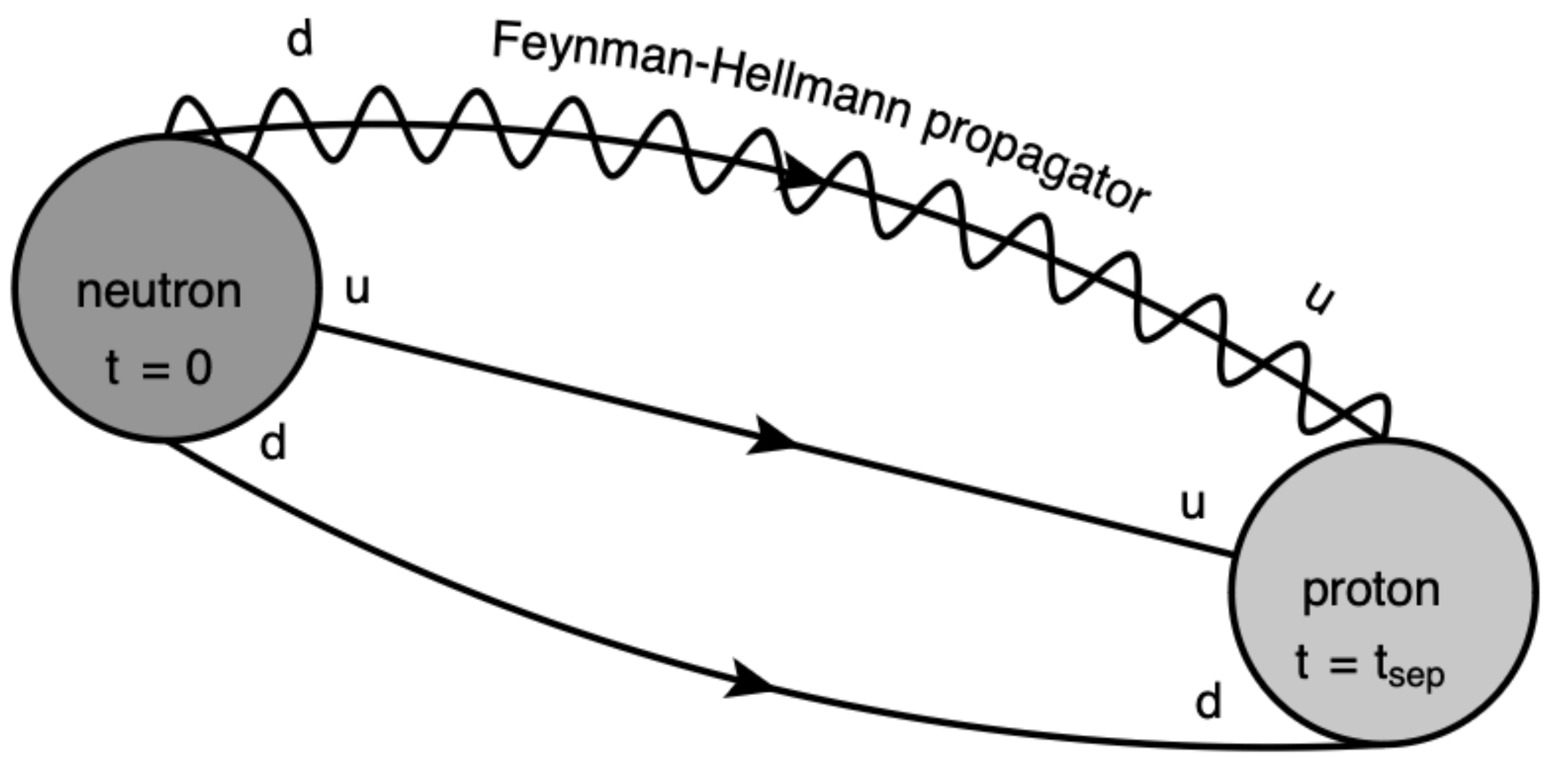

- Build FH correlator vs Ratio

$$\partial_\lambda m^{\text{eff}}_\lambda\,|_{\lambda=0} = \left[\frac{\partial_\lambda C_\lambda(t)}{C(t)} - \frac{\partial_\lambda C_\lambda(t+1)}{C(t+1)}\right]\Bigg|_{\lambda=0} \qquad R_\Gamma(t,\tau) = \frac{C_{3\text{pt}}(t,\tau)}{C_{2\text{pt}}(t)}$$

- FH shows improved control over excited state contamination and cheaper to generate

- Isolate ground state matrix element

$$\lim_{t\to\infty}\partial_\lambda m^{\text{eff}}_\lambda\Big|_{\lambda=0} = g^\Gamma_{00} \qquad \lim_{t\to\infty} R_\Gamma(t,\tau\approx t/2) = g^\Gamma_{00}$$

- See Bouchard et.al PRD 96, 014504 -> FHT and LQCD
- See He et.al PRC 105, 065203 -> 3pt vs FH Excited-State Systematics

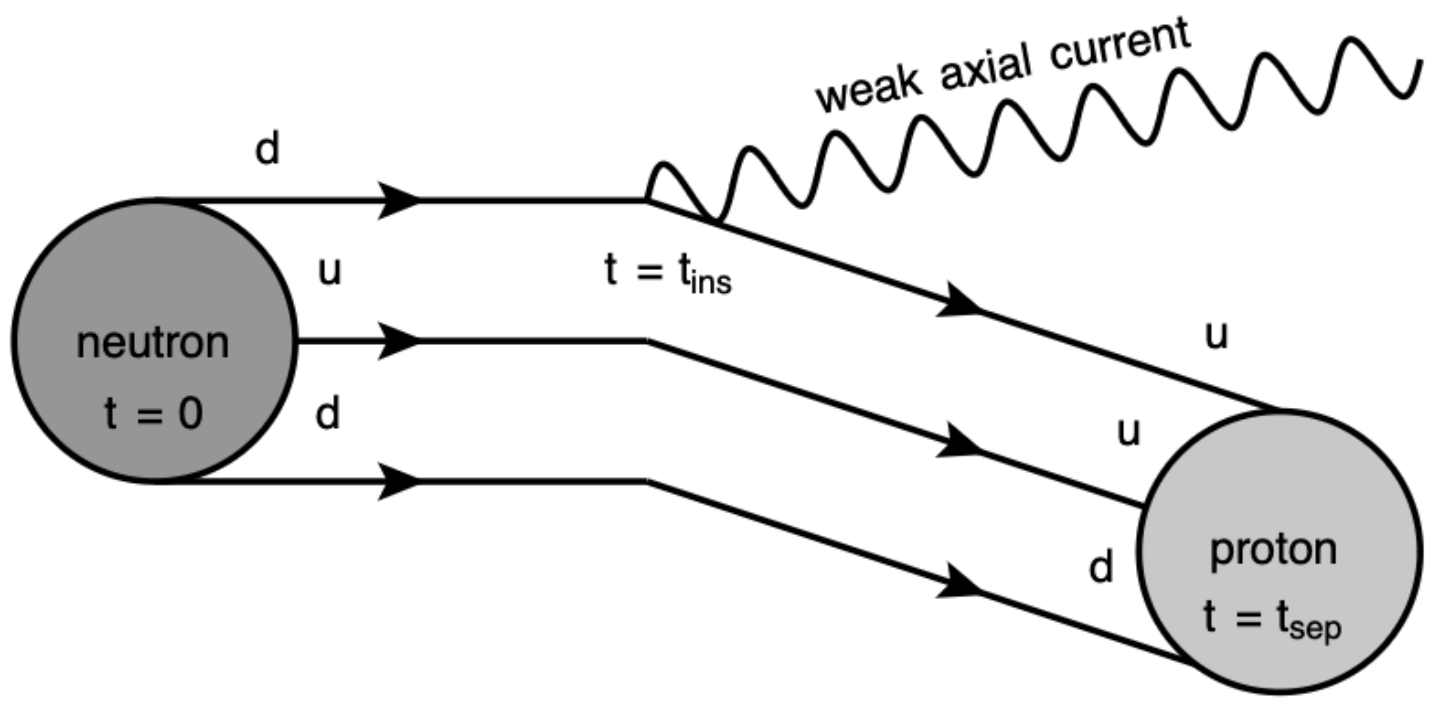

Image credit: Nature 558, 91–94 (2018)

Correlation Functions

$t_{\text{sep}}/a_{09} \in \{2, 3, 4, 5, 6, 7, 8, 9, 10, 11, 12, 13, 14\}$

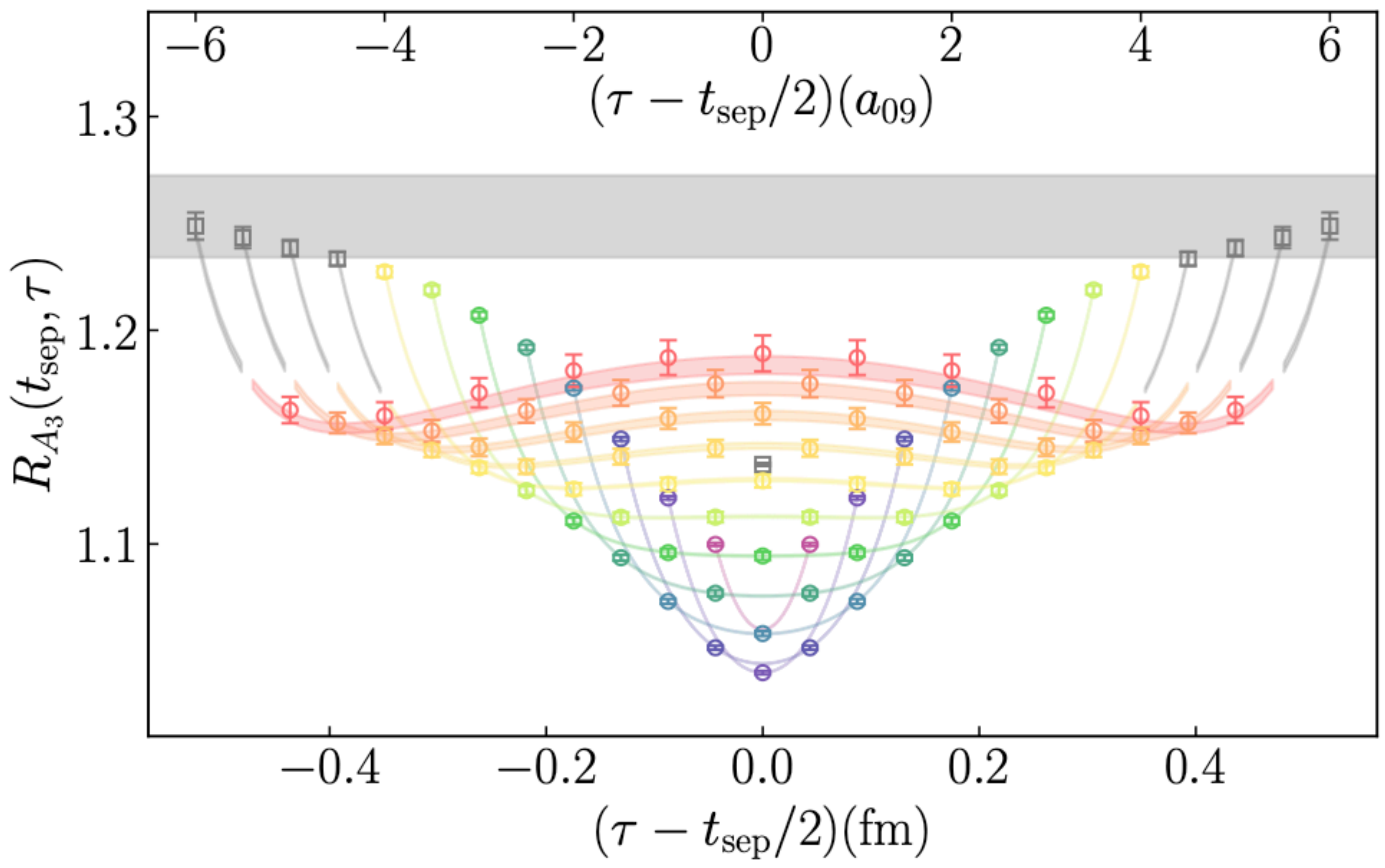

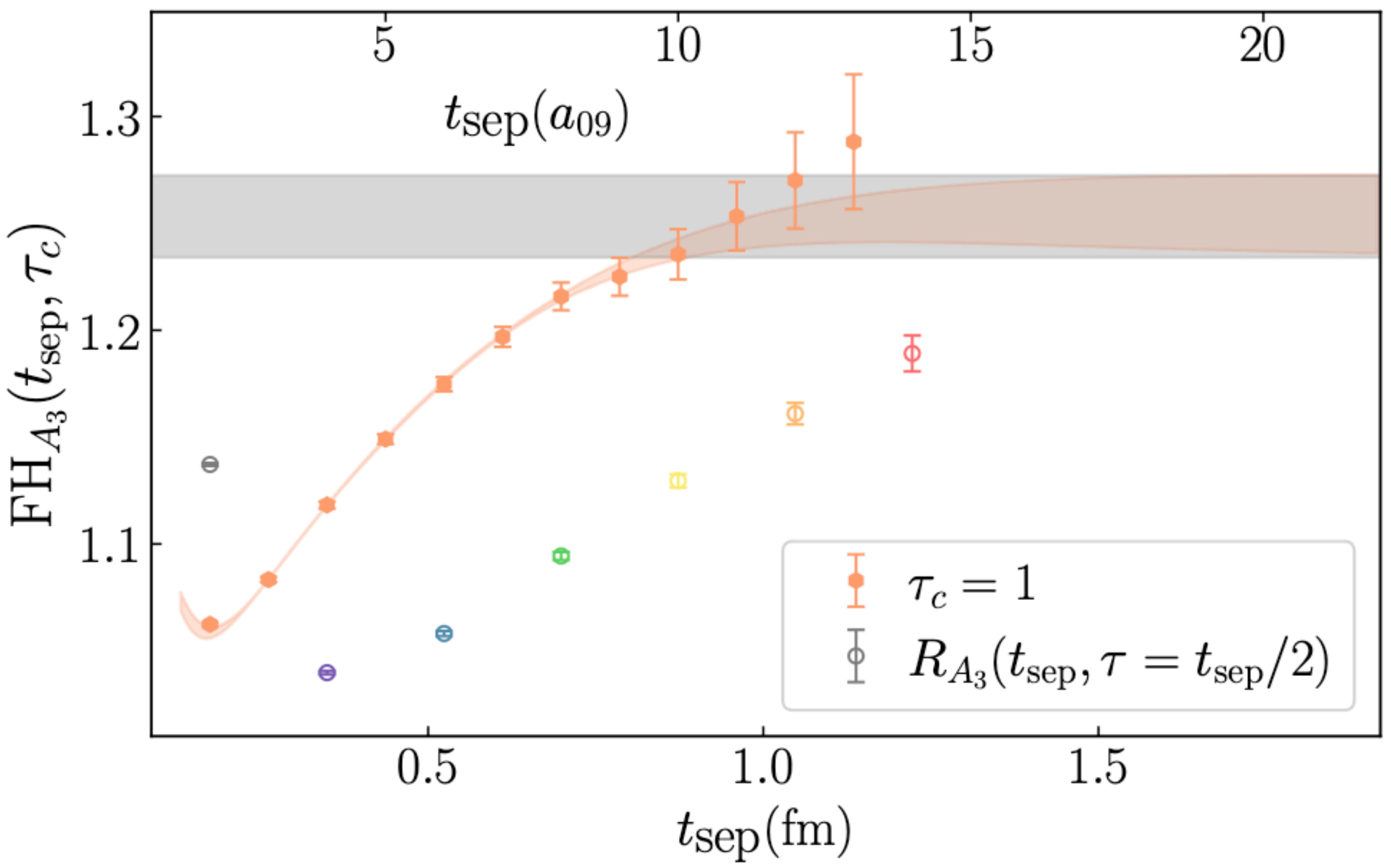

- Example of the Ratio method for many values of t_{sep}.
- Each color represents a different t_{sep} and separate $C_{3\text{pt}}(t_{\text{sep}}, \tau)$ computation.

- Feynman-Hellmann accesses more data at the same computational cost.
- Asymptotes to the ground state matrix element, g_{00} (gray band) at faster than Ratio method.

See Bouchard et.al PRD 96, 014504 -> FHT and LQCD
See He et.al PRC 105, 065203 -> 3pt vs FH Excited-State Systematics

Ensembles and Data

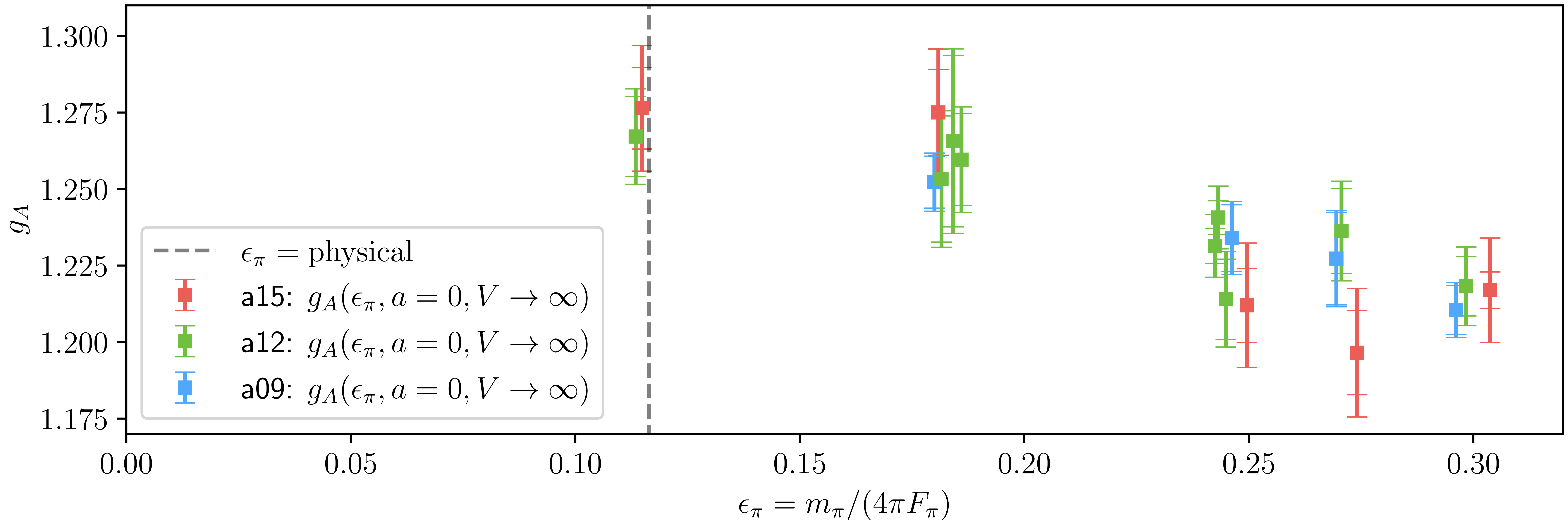

$\epsilon_\pi = \dfrac{m_\pi}{4\pi F_\pi}$ $\quad m_\pi L \quad$ $\epsilon_a = \dfrac{a}{2w_0}$

Need a simultaneous chiral, infinite volume, continuum extrapolation $\rightarrow$ g_A^{phys}

This work: arXiv: 2503.09891 [hep-lat]

*Mixed-Action: Möbius Domain-wall fermions solved on 2+1+1 gradient flowed HISQ ensembles. A subset of HISQ configurations are provided by the MILC collaboration. **New a15m310L,XL

Ensembles and Data

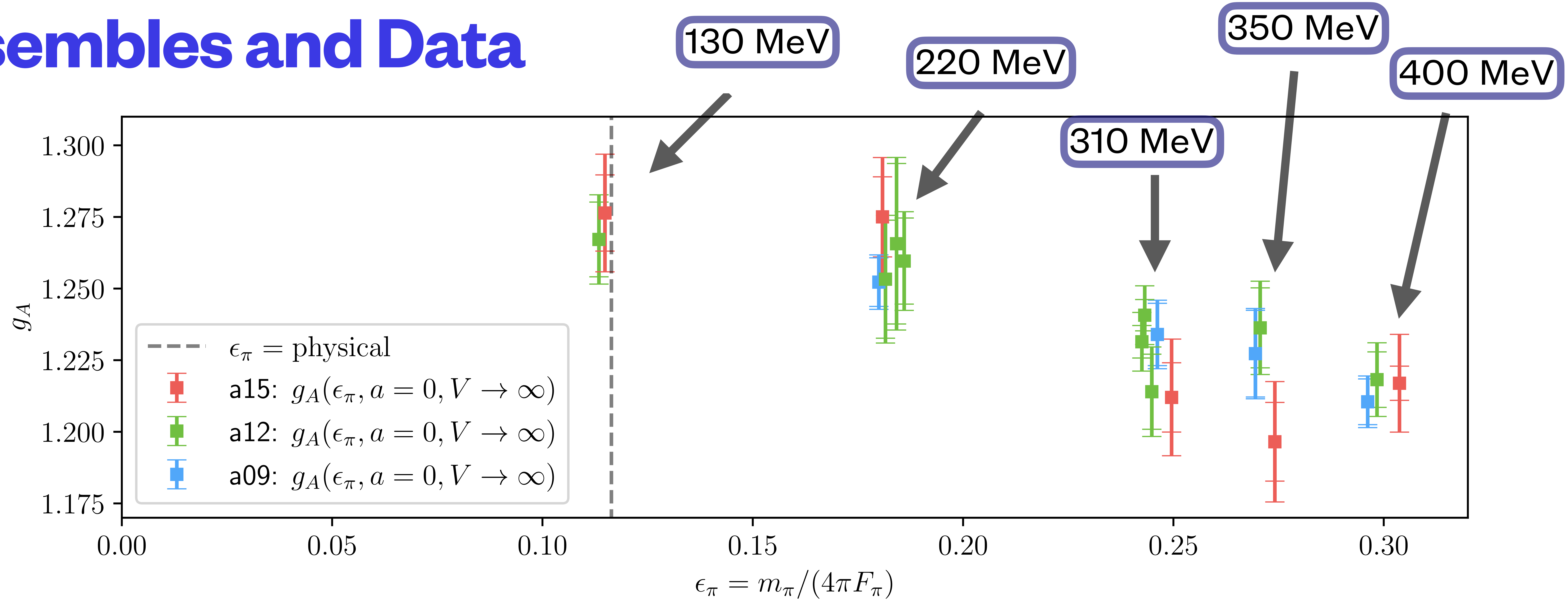

$$\epsilon_\pi = \frac{m_\pi}{4\pi F_\pi}$$

$$m_\pi L$$

$$\epsilon_a = \frac{a}{2w_0}$$

Need a simultaneous chiral, infinite volume, continuum extrapolation $\longrightarrow$ g_A^{phys}

This work: arXiv: 2503.09891 [hep-lat]

*Mixed-Action: Möbius Domain-wall fermions solved on 2+1+1 gradient flowed HISQ ensembles. A subset of HISQ configurations are provided by the MILC collaboration. **New a15m310L,XL

Extrapolation Analysis

- We use a Bayesian framework to perform a nonlinear fitting strategy which extensively utilizes gvar and lsqfit python libraries.
- Agnostic, data-driven approach to determine the model that best represents the data.
- Pion (Quark) mass dependence parameterized through Chiral Perturbation Theory (χPT) up to $O(\epsilon_\pi^3)$:

$$g_{A,\chi} = g_0 + \delta_\chi^{(2)} + \delta_\chi^{(3)}$$

NLO: $$\delta_\chi^{(2)} = \epsilon_\pi^2\left[-(g_0 + 2g_0^3)\ln\epsilon_\pi^2 + \tilde{\mathrm{d}}_{16} - \mathrm{g}_0^3\right]$$

NNLO: $$\delta_\chi^{(3)} = \epsilon_\pi^3 g_0 \frac{2\pi}{3}\left[3(1+g_0^2)\frac{4\pi F_\pi}{M_N} + 4(2\tilde{c}_4 - \tilde{c}_3)\right]$$

- g_0 is the nucleon axial coupling in the chiral limit.

$$\epsilon_\pi = \frac{m_\pi}{4\pi F_\pi} \qquad m_\pi L \qquad \epsilon_a = \frac{a}{2w_0}$$

- Polynomial models:
  - $g_{A,\mathrm{pol}}^{(1)} = c_0 + c_1\epsilon_\pi + c_2\epsilon_\pi^2$
  - $g_{A,\mathrm{pol}}^{(2)} = c_0 + c_2\epsilon_\pi^2 + c_3\epsilon_\pi^3$
  - $g_{A,\mathrm{pol}}^{(3)} = c_0 + c_2\epsilon_\pi^2 + c_4\epsilon_\pi^4$
- We add the finite-volume and lattice spacing effects to each of these models.

https://github.com/gplepage/lsqfit

JHEP 04, 031 (1999), arXiv:hep-ph/9901235 [hep-ph]

Extrapolation Analysis

- We use a Bayesian framework to perform a nonlinear fitting strategy which extensively utilizes gvar and lsqfit python libraries.
- Agnostic, data-driven approach to determine the model that best represents the data.
- Pion (Quark) mass dependence parameterized through Chiral Perturbation Theory (χPT) up to $O(\epsilon_\pi^3)$:

$$g_{A,\chi} = g_0 + \delta_\chi^{(2)} + \delta_\chi^{(3)}$$

NLO: $$\delta_\chi^{(2)} = \epsilon_\pi^2\left[-(g_0 + 2g_0^3)\ln\epsilon_\pi^2 + \tilde{\mathrm{d}}_{16} - \mathrm{g}_0^3\right]$$

NNLO: $$\delta_\chi^{(3)} = \epsilon_\pi^3 g_0 \frac{2\pi}{3}\left[3(1+g_0^2)\frac{4\pi F_\pi}{M_N} + 4(2\tilde{c}_4 - \tilde{c}_3)\right]$$

- g_0 is the nucleon axial coupling in the chiral limit.

$$\epsilon_\pi = \frac{m_\pi}{4\pi F_\pi} \qquad m_\pi L \qquad \epsilon_a = \frac{a}{2w_0}$$

- Polynomial models:
  - $g_{A,\mathrm{pol}}^{(1)} = c_0 + c_1\epsilon_\pi + c_2\epsilon_\pi^2$ Linear
  - $g_{A,\mathrm{pol}}^{(2)} = c_0 + c_2\epsilon_\pi^2 + c_3\epsilon_\pi^3$ "log-less" HBχPT
  - $g_{A,\mathrm{pol}}^{(3)} = c_0 + c_2\epsilon_\pi^2 + c_4\epsilon_\pi^4$ Quadratic
- We add the finite-volume and lattice spacing effects to each of these models.

https://github.com/gplepage/lsqfit

JHEP 04, 031 (1999), arXiv:hep-ph/9901235 [hep-ph]

Extrapolation Analysis

- We use a Bayesian framework to perform a nonlinear fitting strategy which extensively utilizes gvar and lsqfit python libraries.
- Agnostic, data-driven approach to determine the model that best represents the data.
- Pion (Quark) mass dependence parameterized through Chiral Perturbation Theory (χPT) up to $O(\epsilon_\pi^3)$:

$$g_{A,\chi} = g_0 + \delta_\chi^{(2)} + \delta_\chi^{(3)}$$

NLO: $$\delta_\chi^{(2)} = \epsilon_\pi^2\left[-(g_0 + 2g_0^3)\ln\epsilon_\pi^2 + \tilde{\mathrm{d}}_{16} - \mathrm{g}_0^3\right]$$

NNLO: $$\delta_\chi^{(3)} = \epsilon_\pi^3 g_0 \frac{2\pi}{3}\left[3(1+g_0^2)\frac{4\pi F_\pi}{M_N} + 4(2\tilde{c}_4 - \tilde{c}_3)\right]$$

- g_0 is the nucleon axial coupling in the chiral limit.

$$\epsilon_\pi = \frac{m_\pi}{4\pi F_\pi} \qquad m_\pi L \qquad \epsilon_a = \frac{a}{2w_0}$$

- Polynomial models:
  - $g_{A,\mathrm{pol}}^{(1)} = c_0 + c_1\epsilon_\pi + c_2\epsilon_\pi^2$ Linear
  - $g_{A,\mathrm{pol}}^{(2)} = c_0 + c_2\epsilon_\pi^2 + c_3\epsilon_\pi^3$ “log-less” HBχPT
  - $g_{A,\mathrm{pol}}^{(3)} = c_0 + c_2\epsilon_\pi^2 + c_4\epsilon_\pi^4$ Quadratic
- We add the finite-volume and lattice spacing effects to each of these models.

https://github.com/gplepage/lsqfit

JHEP 04, 031 (1999), arXiv:hep-ph/9901235 [hep-ph]

Extrapolation Results

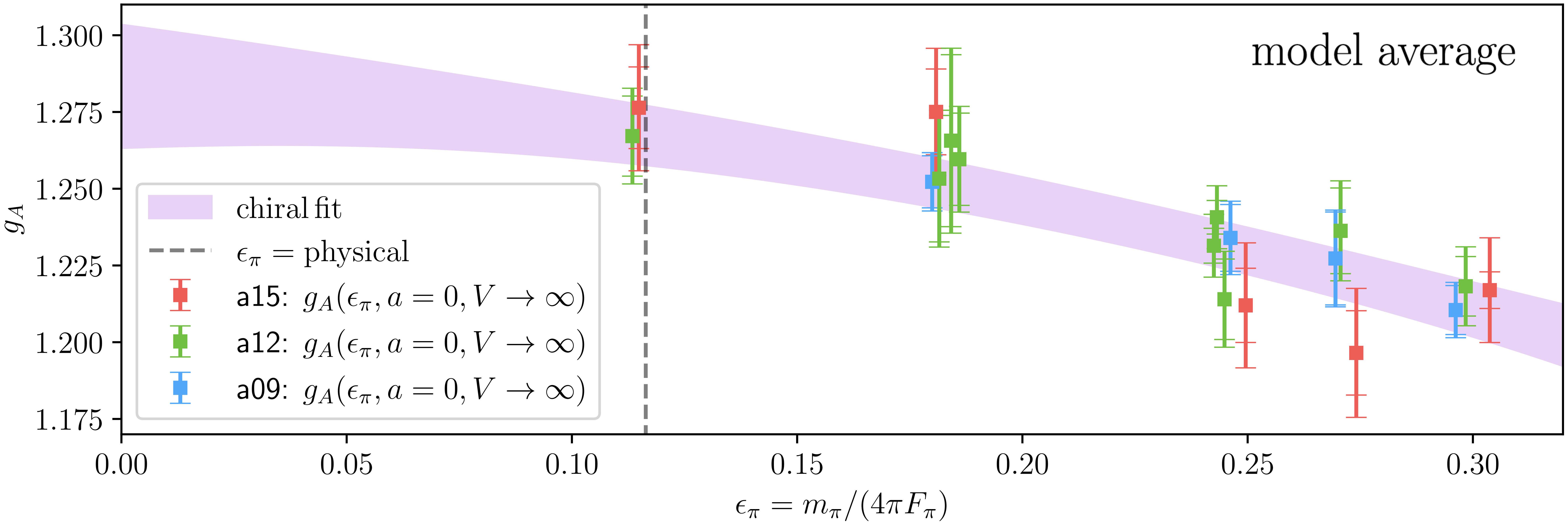

- Chiral-continuum-IV fits for 64 models over all 18 ensembles.

$$g_A = 1.2674(79)^{\mathrm{s}}(28)^{\chi}(05)^{\mathrm{FV}}(38)^{a}(26)^{\mathrm{M}}$$
$$= 1.2674(96)$$

statistical	0.62%
chiral	0.22%
finite volume	0.06%
continuum	0.30%
model	0.20%
total	0.76%

$$g_A^{\mathrm{PDG}} = 1.2754(13)$$

This work: arXiv: 2503.09891 [hep-lat]

Extrapolation Results

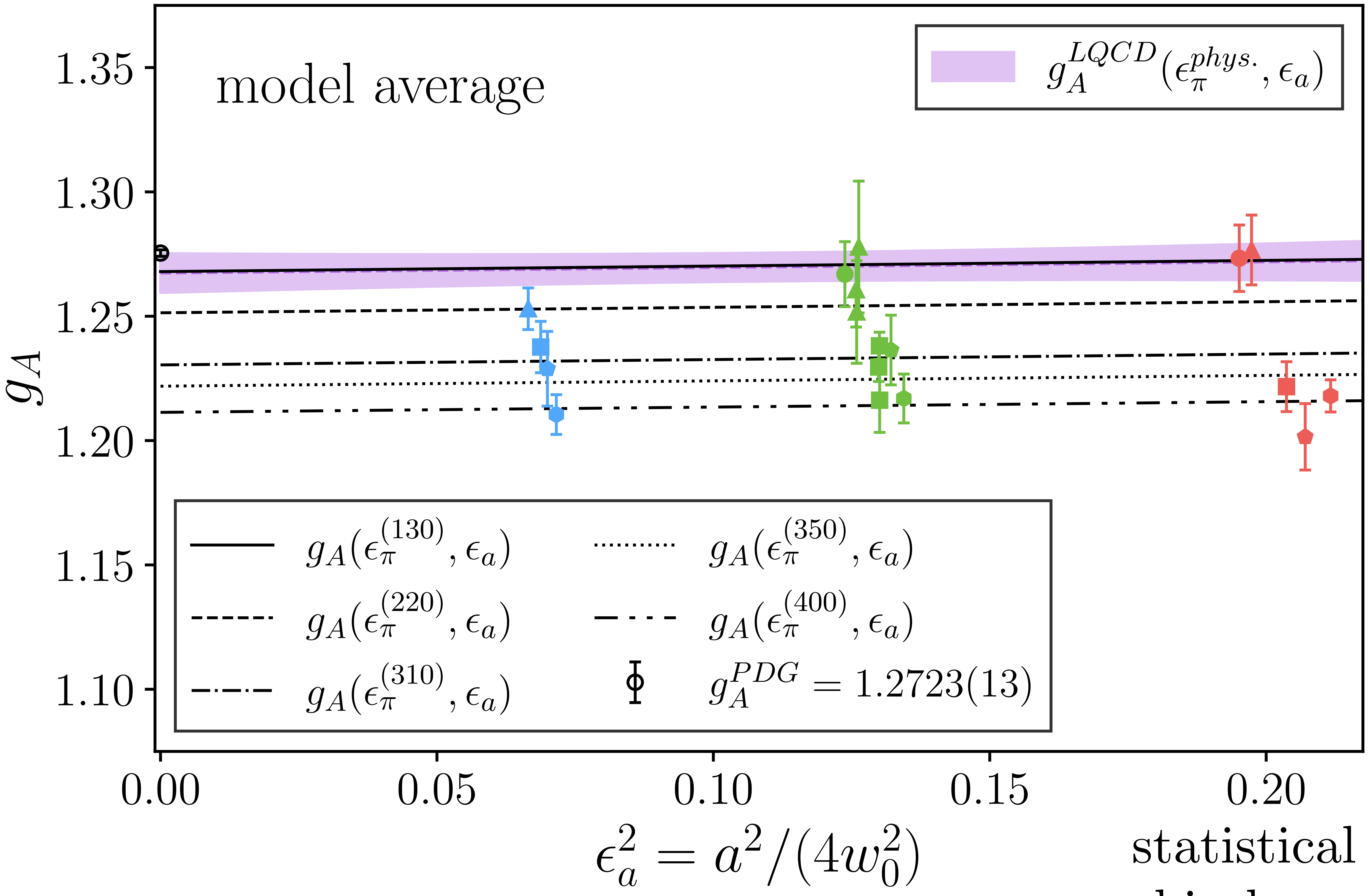

statistical	0.62%
chiral	0.22%
finite volume	0.06%
continuum	0.30%
model	0.20%
total	0.76%

- Chiral-continuum-IV fits for 64 models over all 18 ensembles.

$$g_A = 1.2674(79)^{\mathrm{s}}(28)^{\chi}(05)^{\mathrm{FV}}(38)^{a}(26)^{\mathrm{M}}$$
$$= 1.2674(96)$$

$$g_A^{\mathrm{PDG}} = 1.2754(13)$$

This work: arXiv: 2503.09891 [hep-lat]

Extrapolation Results

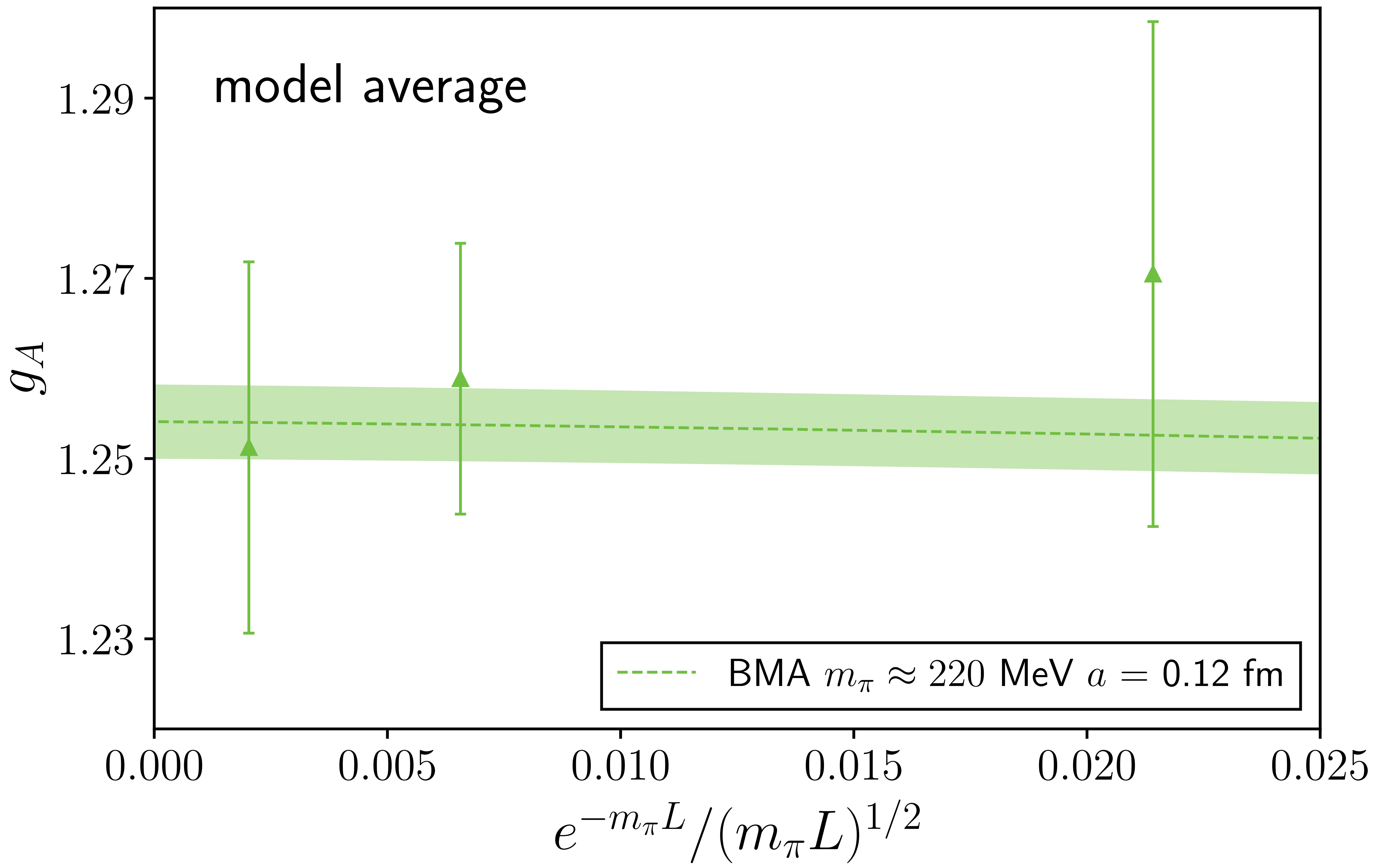

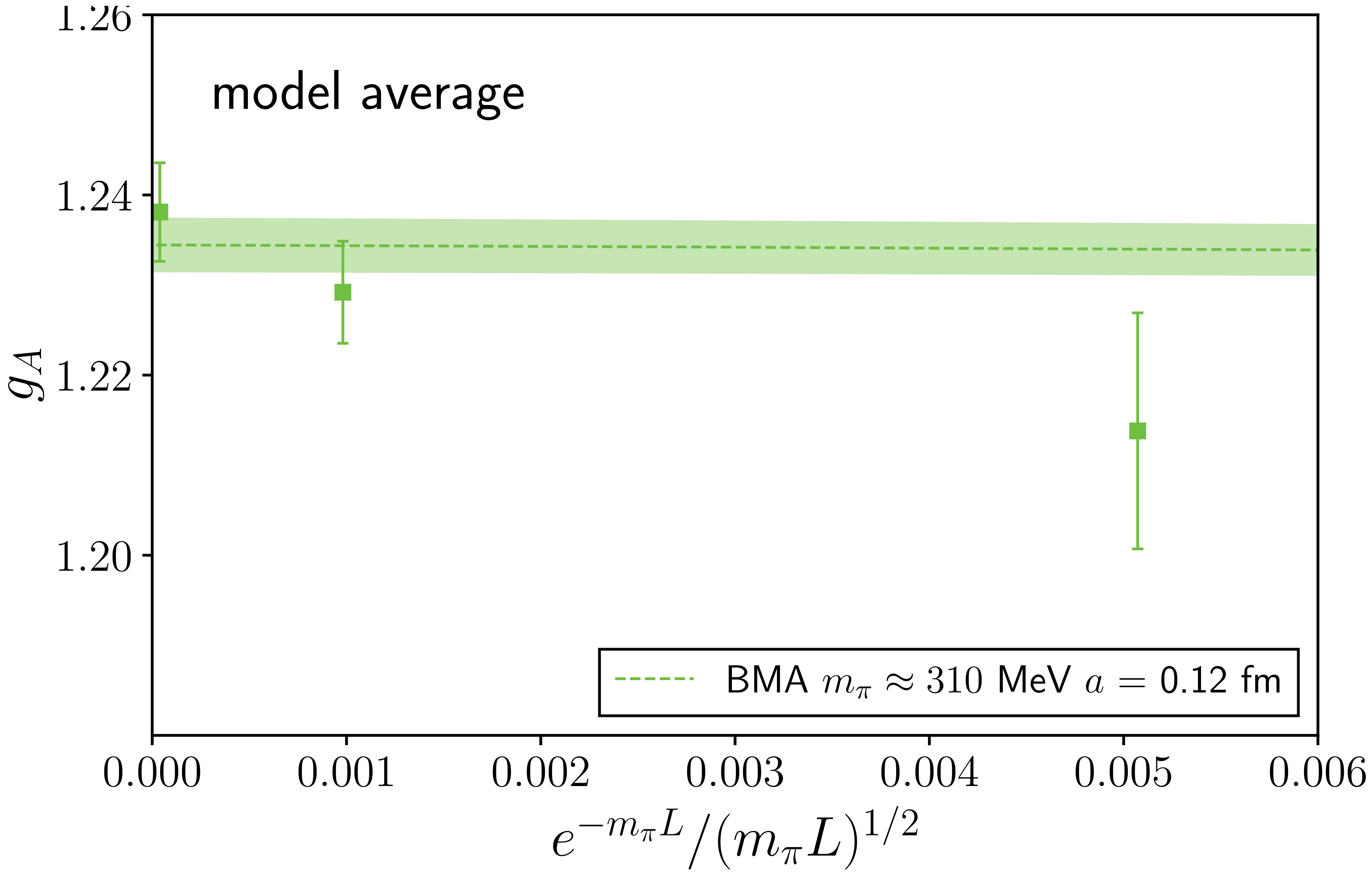

statistical	0.62%
chiral	0.22%
finite volume	0.06%
continuum	0.30%
model	0.20%
total	0.76%

- Chiral-continuum-IV fits for 64 models over all 18 ensembles.

$$g_A = 1.2674(79)^{\mathrm{s}}(28)^{\chi}(05)^{\mathrm{FV}}(38)^{a}(26)^{\mathrm{M}} = 1.2674(96)$$

$$g_A^{\mathrm{PDG}} = 1.2754(13)$$

This work: arXiv: 2503.09891 [hep-lat]

Extrapolation Results

$$g_A = 1.2674(79)^{s}(28)^{\chi}(05)^{FV}(38)^{a}(26)^{M}$$
$$= 1.2674(96)$$

- First LQCD determination of g_A at the sub-percent level in the isospin limit, fully accounting for systematics.
- Performed detailed FV study.

$$g_A^{\mathrm{non-mon}} = 1.2672(96) \qquad g_A^{\mathrm{mon}} = 1.2674(96)$$

- In the BMA, Polynomial models are highly preferred over all χPT.
- See paper for discussion on the impact of Δ-baryon on interpretation of FV and on the convergence of g_A.

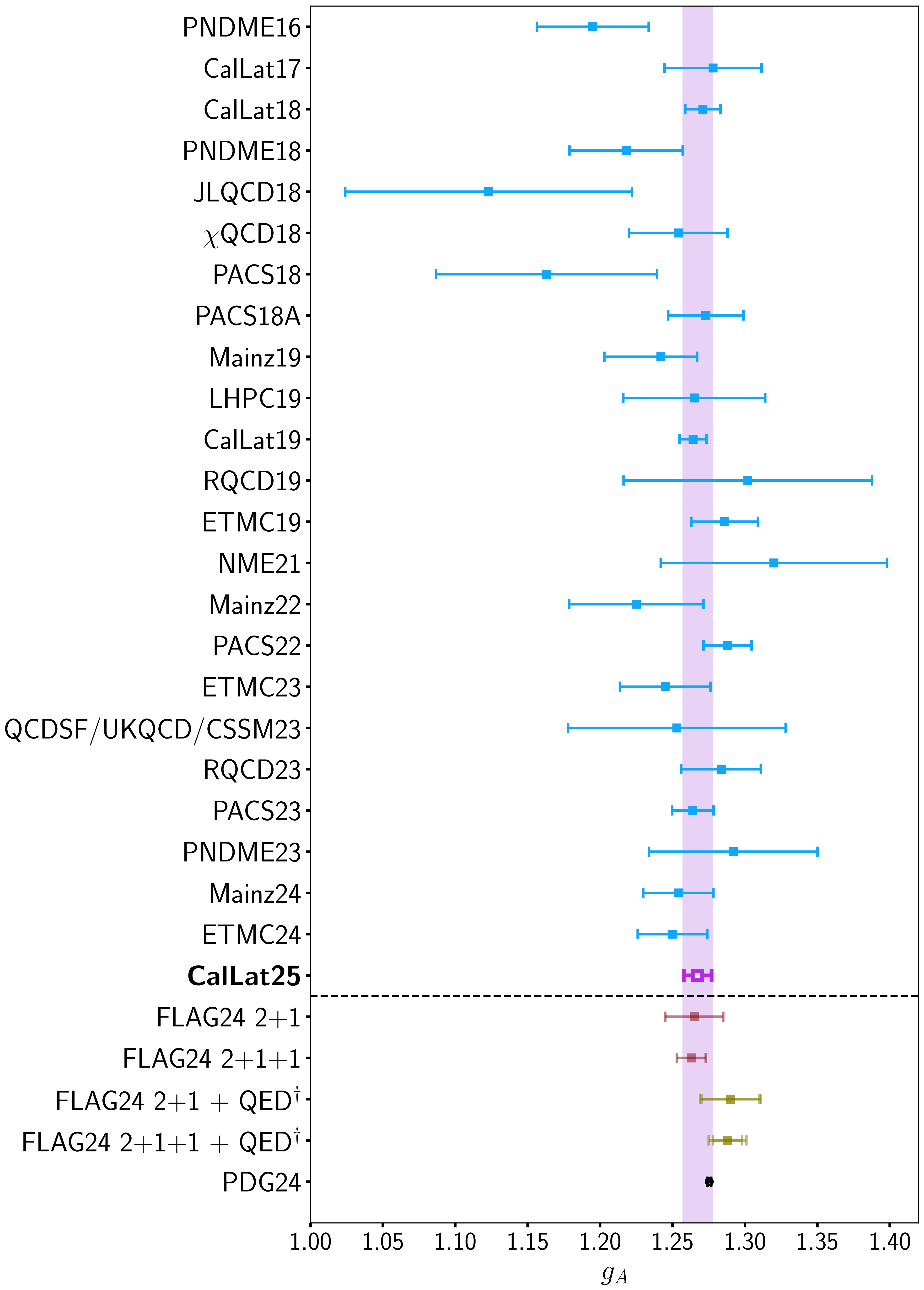

This work: arXiv: 2503.09891 [hep-lat]

Outlook and Summary for g_A

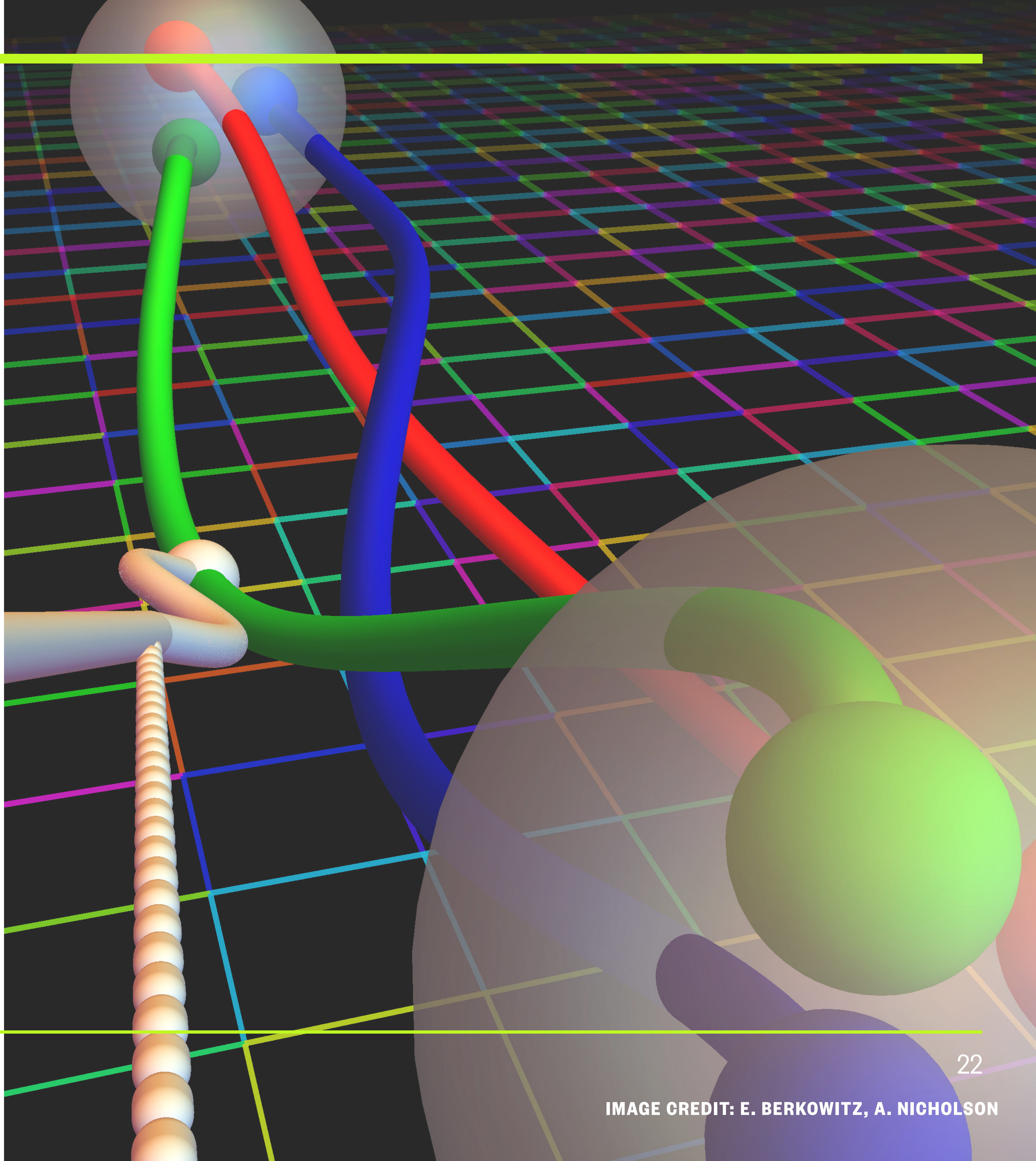

IMAGE CREDIT: E. BERKOWITZ, A. NICHOLSON

RE: Low-Energy Precision Physics

- We can precisely calculate g_A with LQCD:

$$g_A \sim \langle p | \bar{u}\gamma^3\gamma^5 d | n \rangle$$

- We have g_A at sub-percent level with pure QCD -> EFT estimates QED effects at O(2%)
  - LQCD+QED -> isolate these two SM contributions (strong + radiative corrections)
- Uncertainty in V_{ud} is inhibited by λ, on the theory side, currently g_A lacks QED corrections.
- This research is part of a larger program for building the theoretical and computational framework for $g_A^{\text{QCD+QED}}$.
  - LQCD+QED underway for simple observables.

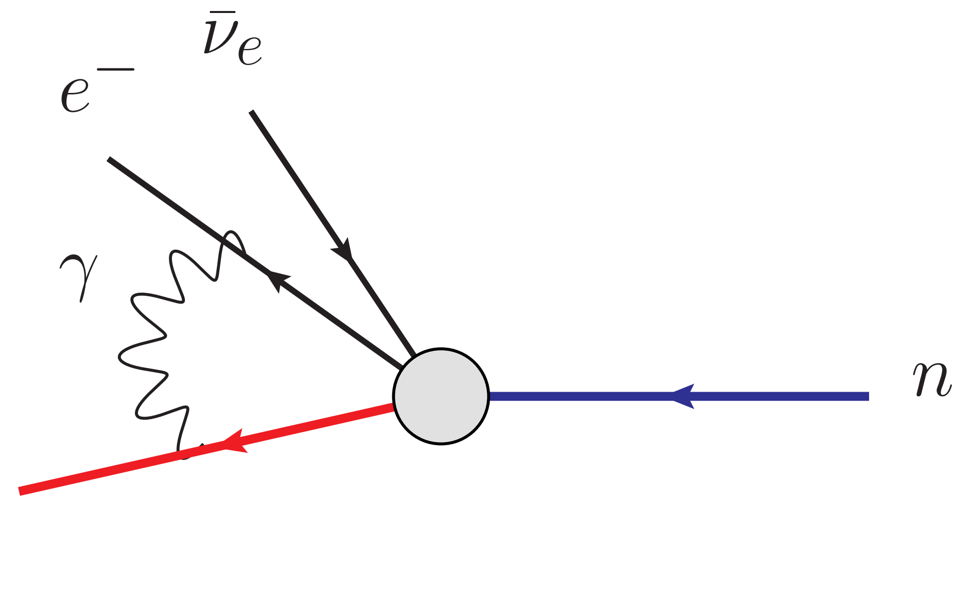

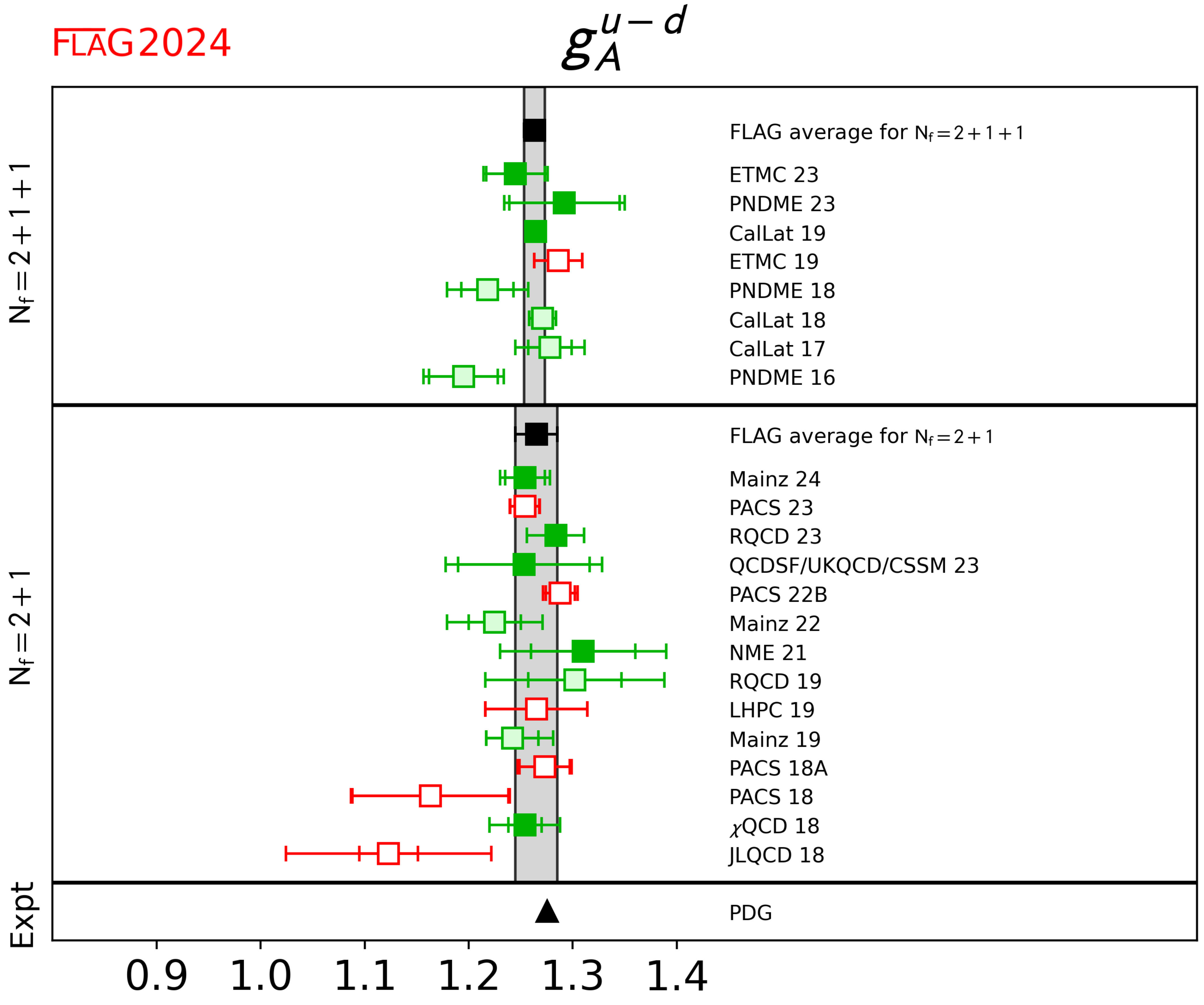

Image credit: Vincenzo Cirigliano

This work: arXiv: 2503.09891 [hep-lat]
EFT: PRL 129, 121801 [2202.10439]
LQCD + QED: arXiv:2201.03251v1

Outlook - BSM Physics

JHEP 03 (2024) [2311.00021]

- Already, g_A at 1% sets constraints on BSM right-handed charge currents (RHCC).

- A recent study considers high-energy collider observables, low-energy charged current processes, and electroweak precision observables within a SMEFT framework.

$$g_A = g_A^{\text{QCD}}\left(1 + \delta_{\text{RC}}^{g_A} - 2\text{Re}(\epsilon_{\text{R}})\right)$$

$$\left.\begin{aligned} g_A &= 1.2754(13) \\ g_A^{\text{QCD}} &= 1.2674(96) \\ \delta_{\text{RC}}^{g_A} &\in \{0.014,\ 0.026\} \end{aligned}\right\} \longrightarrow \text{Re}(\epsilon_{\text{R}})$$

Can be estimated

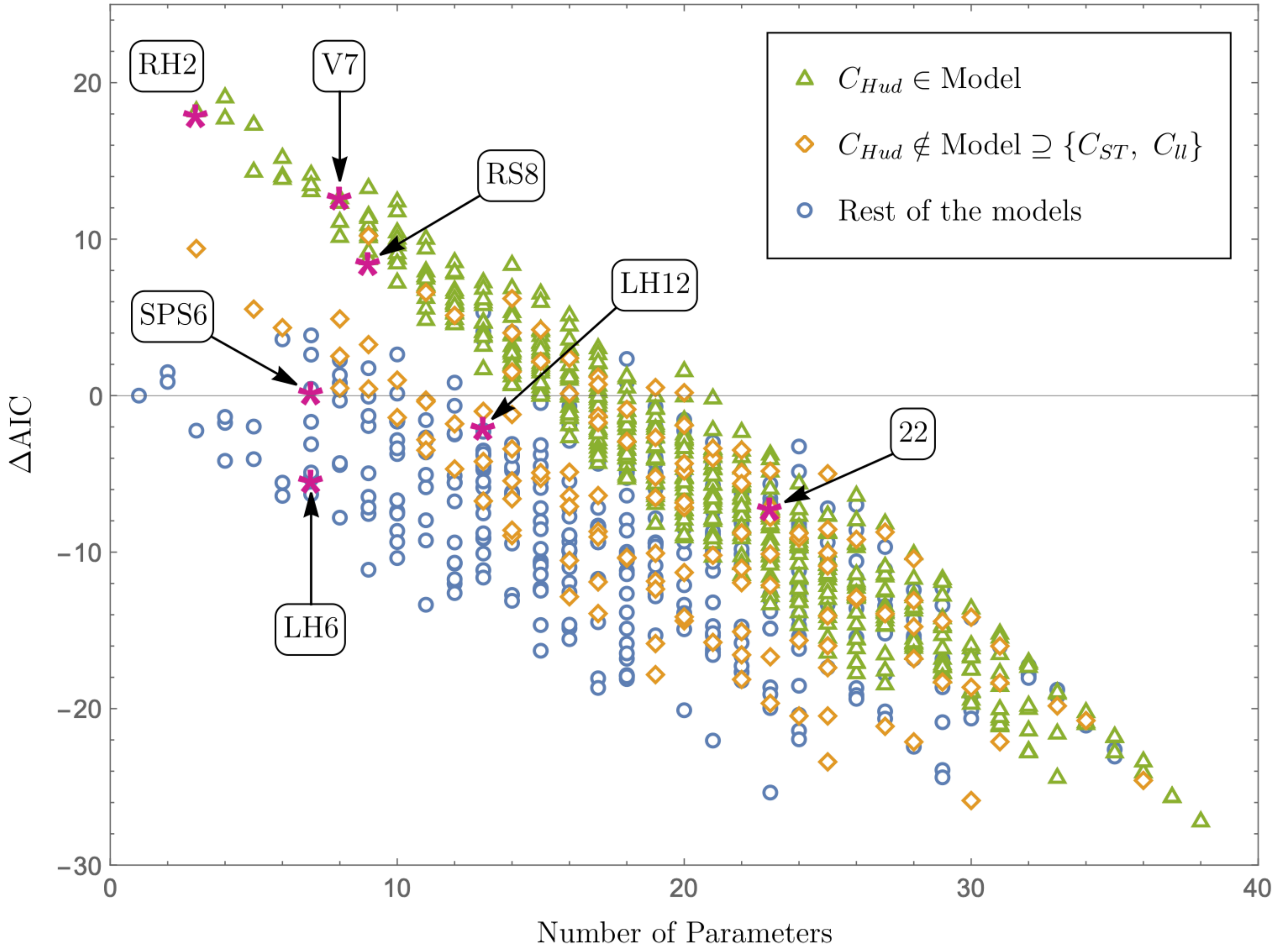

- This global analysis shows that BSM models including RHCC are strongly favored and could alleviate the tension in CKM unitarity.

$$\Delta_{\text{CKM}} = |V_{ud}|^2 + |V_{us}|^2 + |\cancel{V_{ub}}|^2 - 1$$
$$= -0.00176(56)$$

- The Cabibbo Angle Anomaly could be explained by these RHCC but need both g_A^{QCD} and $\delta_{\text{RC}}^{g_A}$ at the sub-percent level -> motivating the need for $g_A^{\text{QCD+QED}}$ from the lattice.

$\delta_{RC}^{g_A}$ from PRL 129, 121801 [2202.10439]

Acknowledgements

California Lattice Collaboration

*Not all in California

Nuclear Theory for New Physics
co-chairs: *Vincenzo Cirigliano & Saori Pastore*

DEI Coordinator: *Maria Piarulli*

Lattice QCD
Coordinator:
Andre' Walker-Loud

EFT / phenomenology
Coordinator:
Emanuele Mereghetti

Nuclear Structure
Coordinator:
Heiko Hergert

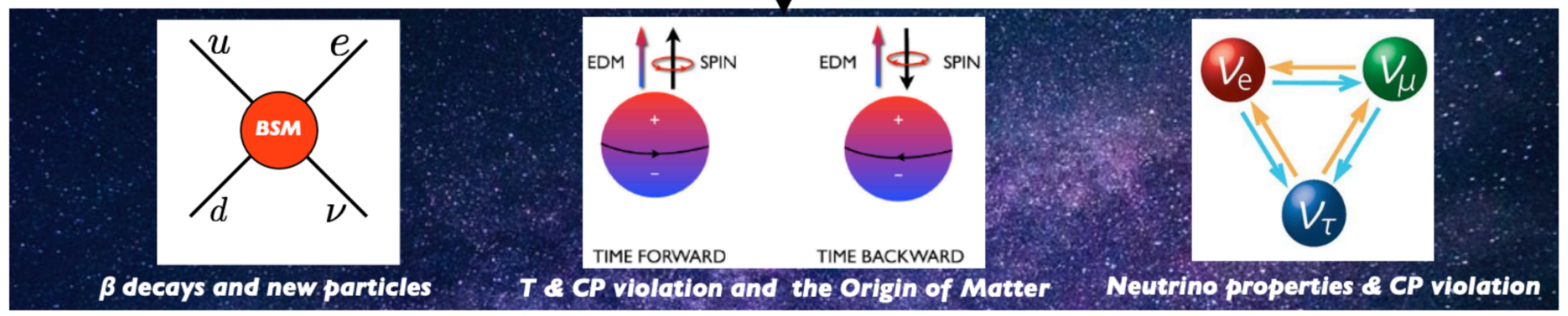

Collaborators

André Walker-Loud	LBNL/UC Berkeley
Dimitra Pefkou	UC Berkeley/LBNL
Thomas Richardson	UC Berkeley/LBNL
Amy Nicholson	UNC Chapel Hill
Henry Monge-Camacho	ORNL
Aaron Meyer	LLNL
Kate Clark	Nvidia
Raúl Briceño	UC Berkeley/LBNL
Emmanuelle Mereghetti	LANL
Martin Hoferichter	University of Bern
Pavlos Vranas	LLNL

U.S. DEPARTMENT OF ENERGY | Office of Science

BERKELEY LAB
Bringing Science Solutions to the World

NSF

THE UNIVERSITY of NORTH CAROLINA at CHAPEL HILL

Office of Science
Graduate Student Research Program

Extra Slides

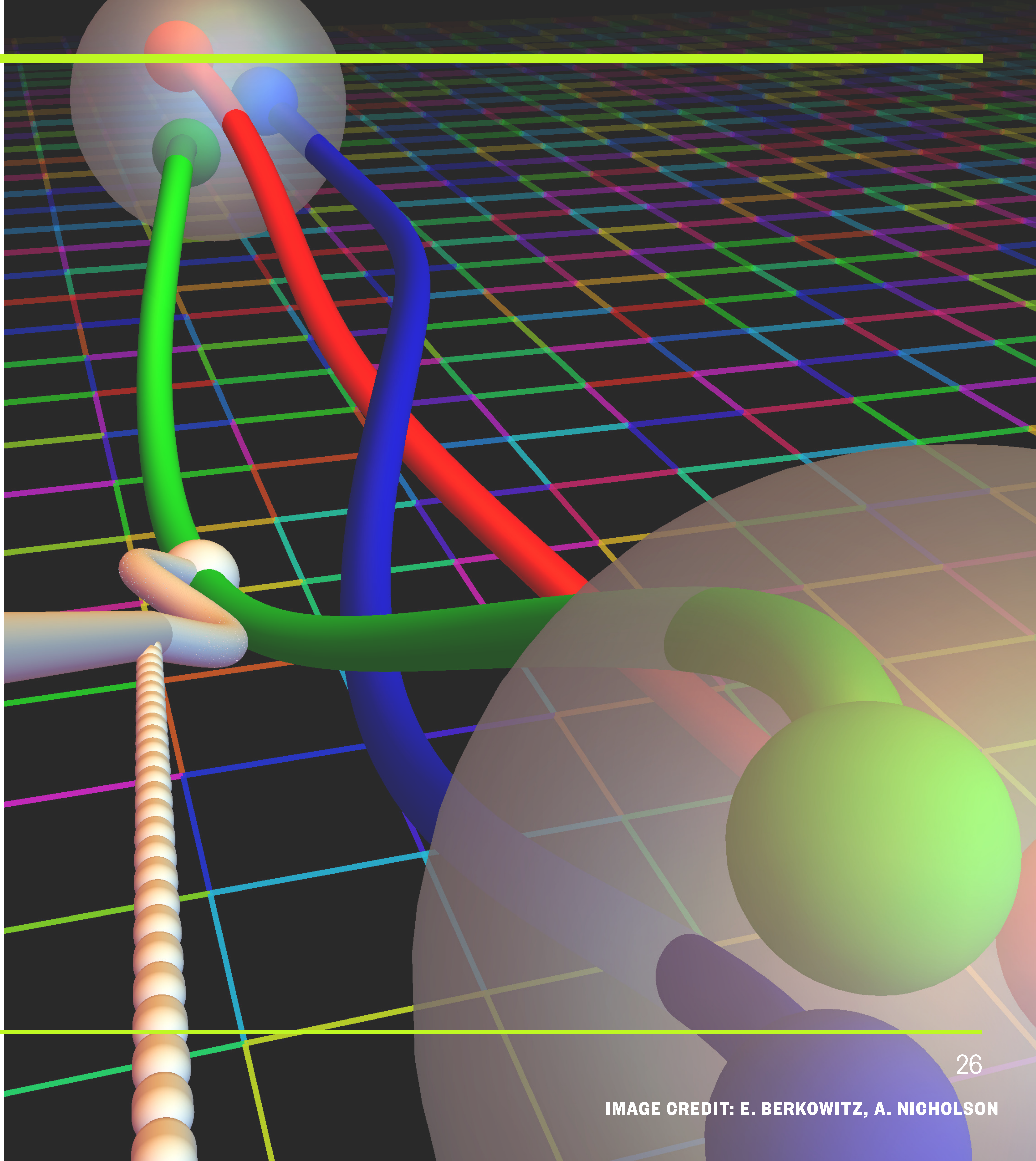

IMAGE CREDIT: E. BERKOWITZ, A. NICHOLSON

Low-Energy Precision Physics

- The top-row Cabbibo-Kabayashi-Maskawa (CKM) matrix unitarity test is one of the most sensitive probes of BSM physics in the low-energy regime.

$$\begin{pmatrix} d \\ s \\ b \end{pmatrix}_{\text{Weak}} = \underbrace{\begin{pmatrix} V_{ud} & V_{us} & V_{ub} \\ V_{cd} & V_{cs} & V_{cb} \\ V_{td} & V_{ts} & V_{tb} \end{pmatrix}}_{\text{CKM}} \begin{pmatrix} d \\ s \\ b \end{pmatrix}_{QCD}$$

$$\begin{aligned} \Delta_{\text{CKM}} &= |V_{ud}|^2 + |V_{us}|^2 + \cancel{|V_{ub}|^2} - 1 \\ &= -0.00176(56) \end{aligned}$$

$$|V_{ub}|^2 \sim O(10^{-5})$$

- 3σ deficit away from unitarity

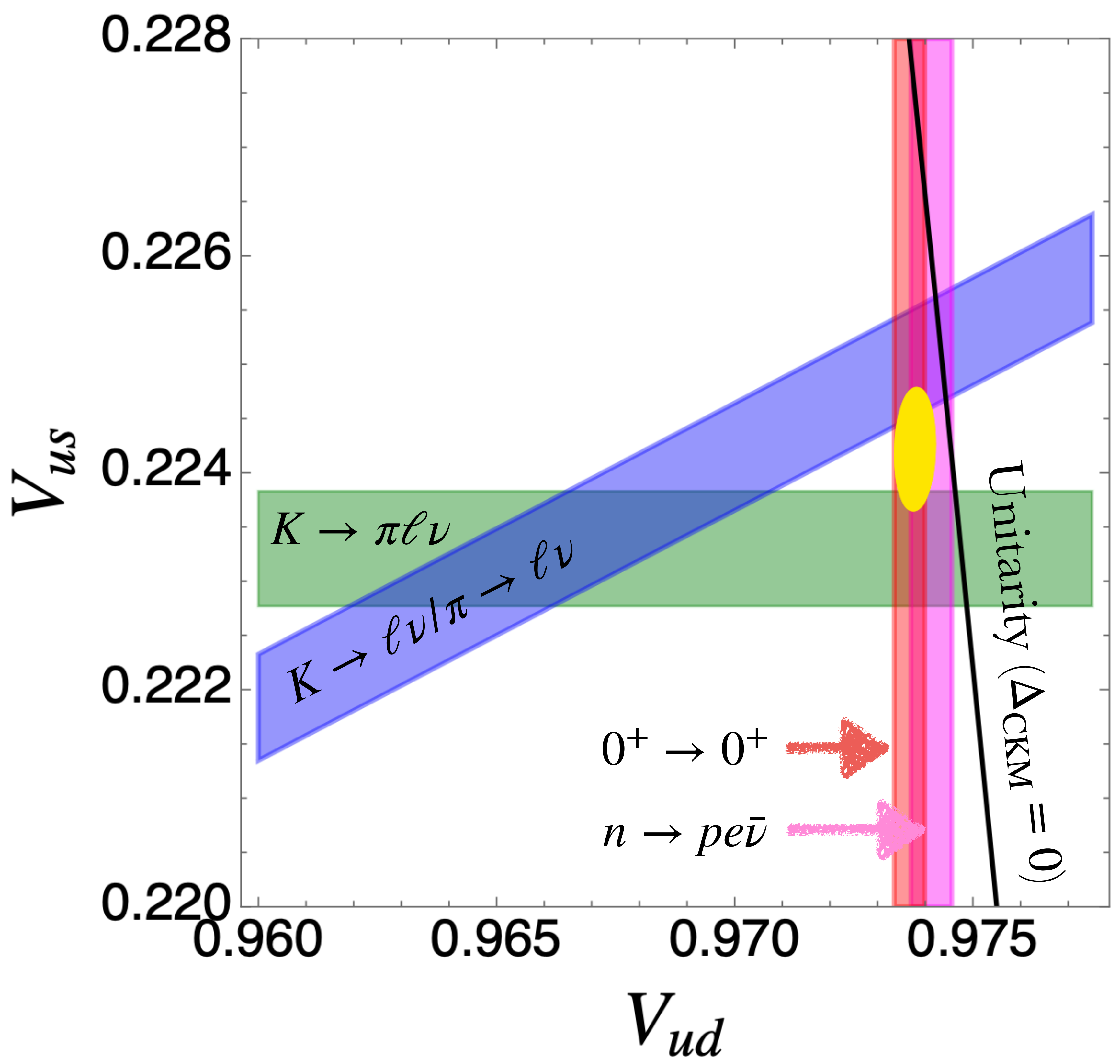

- $K_{\ell 2}/\pi_{\ell 2} \sim V_{us}/V_{ud}$, can be calculated from exp and theory
- $K_{\ell 3} \sim V_{us}$, determined from exp, full theory underway
- $0^+ \to 0^+ \sim V_{ud}$, most precise but inhibited by NS corrections
- $n \to pe\nu \sim V_{ud}$, becoming a competitive approach

$$V_{us}/V_{ud} = 0.23108(23)_{\text{exp}}(42)_{F_K/F_\pi}(16)_{\text{IB}}[51]_{\text{total}}$$

$$V_{us} = 0.22330(35)_{\text{exp}}(39)_{f_+}(8)_{\text{IB}}[53]_{\text{total}}$$

$$V_{ud}^{0^+\to 0^+} = 0.97367(11)_{\text{exp}}(13)_{\Delta_V^R}(27)_{\text{NS}}[32]_{\text{total}}$$

$$V_{ud}^{n,\text{PDG}} = 0.97441(3)_f(13)_{\Delta_V^R}(82)_\lambda(28)_{\tau_n}[88]_{\text{total}}$$

Phys. Lett. B 838 (2023) 137748, arXiv:2208.11707

Correlation Functions

- Matrix Elements

$$C_{3\text{pt}}(t,\tau) = \sum_{\mathbf{x},\mathbf{y}} \langle O(t,\mathbf{y})\, J^{\Gamma}(\tau,\mathbf{x})\, O^{\dagger}(0,\mathbf{0})\rangle$$

- Inserting a complete set of states

$$1 = \sum_n |n\rangle\langle n| \qquad 1 = \sum_m |m\rangle\langle m|$$

$$C_{3\text{pt}}(t,\tau) = \sum_n |A_n|^2\, g^{\Gamma}_{nn}\, e^{-E_n t} + 2\sum_{n<m} A_n A^{\dagger}_m\, g^{\Gamma}_{nm}\, e^{(-E_n+\Delta_{nm}/2)t}\, \cosh\!\left[\Delta_{mn}\left(\tau - \frac{t}{2}\right)\right]$$

$$A_n = \langle n|O^{\dagger}|\Omega\rangle \qquad g^{\Gamma}_{mn} = \langle m|J^{\Gamma}|n\rangle$$

- Isolate ground state matrix element

$$R_{\Gamma}(t,\tau) = \frac{C_{3\text{pt}}(t,\tau)}{C_{2\text{pt}}(t)} \longrightarrow \lim_{t\to\infty} R_{\Gamma}(t,\tau\approx t/2) = g^{\Gamma}_{00}$$

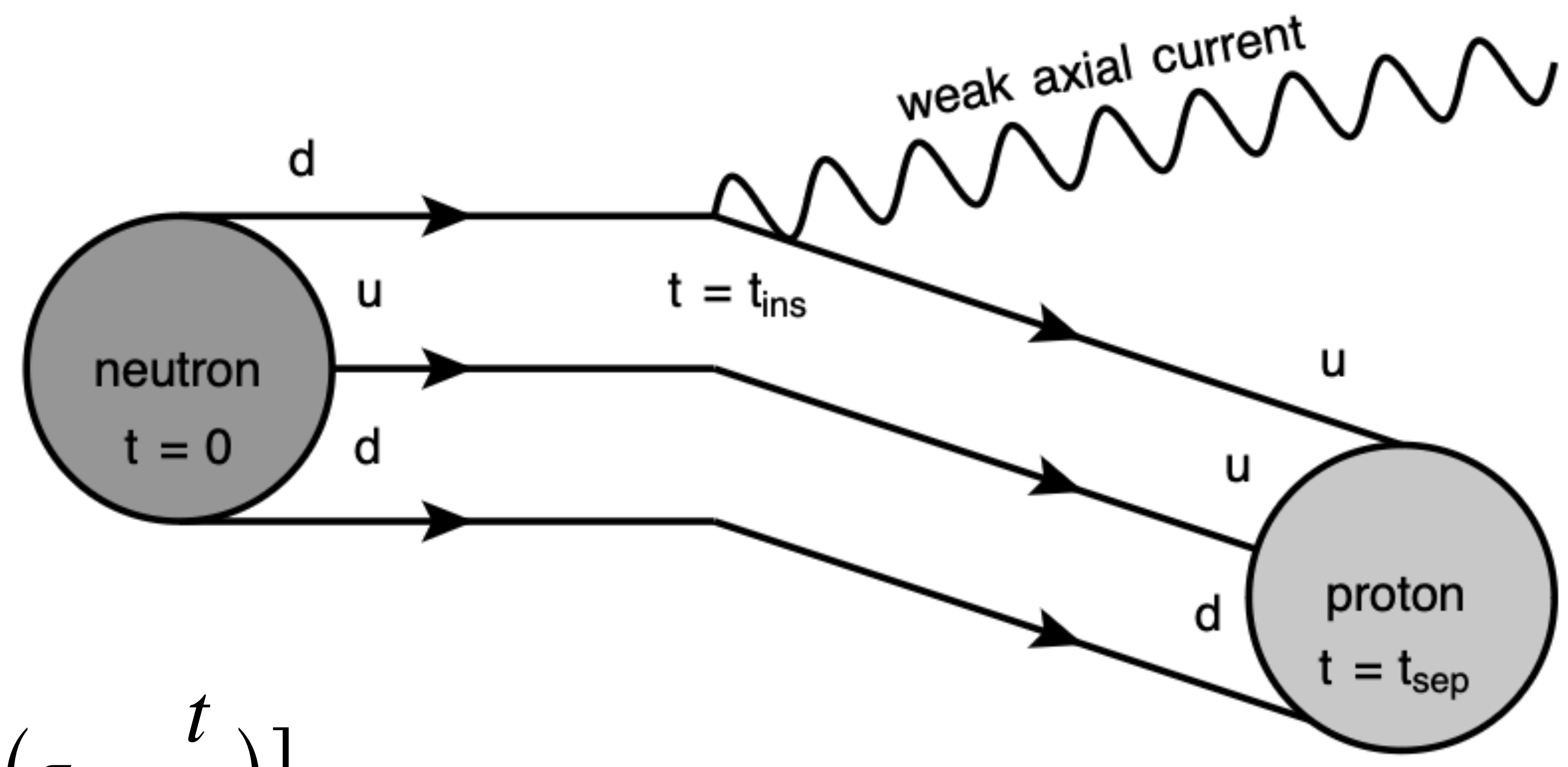

- Challenges: computationally expensive to reduce excited state contamination and difficult to characterize

Image credit: Nature 558, 91–94 (2018)

Correlation Functions

- Feynman-Hellmann Inspired Approach

$$\frac{\partial E_n}{\partial \lambda} = \langle n | H_\lambda | n \rangle \qquad H = H_0 + \lambda H_\lambda$$

- 2pt in the presence of external source

$$C_\lambda(t) = \langle \lambda | O(t)\, O^\dagger(0) | \lambda \rangle = \frac{1}{Z_\lambda} \int D[\Phi]\, \mathrm{e}^{-S-S_\lambda}\, O(t)\, O^\dagger(0)$$

$$-\partial_\lambda C_\lambda(t)\big|_{\lambda=0} = \int d\tau\, \langle \Omega | T\{O(t)\, J(\tau)\, O^\dagger(0)\} | \Omega \rangle = \sum_{\tau}^{t} C_{3\mathrm{pt}}(t,\tau)$$

- Apply FHT to effective mass

$$m^{\mathrm{eff}} = \ln\left(\frac{C(t)}{C(t+1)}\right) \rightarrow \partial_\lambda m_\lambda^{\mathrm{eff}}\big|_{\lambda=0} = \left[\frac{\partial_\lambda C_\lambda(t)}{C(t)} - \frac{\partial_\lambda C_\lambda(t+1)}{C(t+1)}\right]\Bigg|_{\lambda=0}$$

- Isolate ground state matrix element

$$\lim_{t\to\infty} \partial_\lambda m_\lambda^{\mathrm{eff}}\Big|_{\lambda=0} = g_{00}^{\Gamma}$$

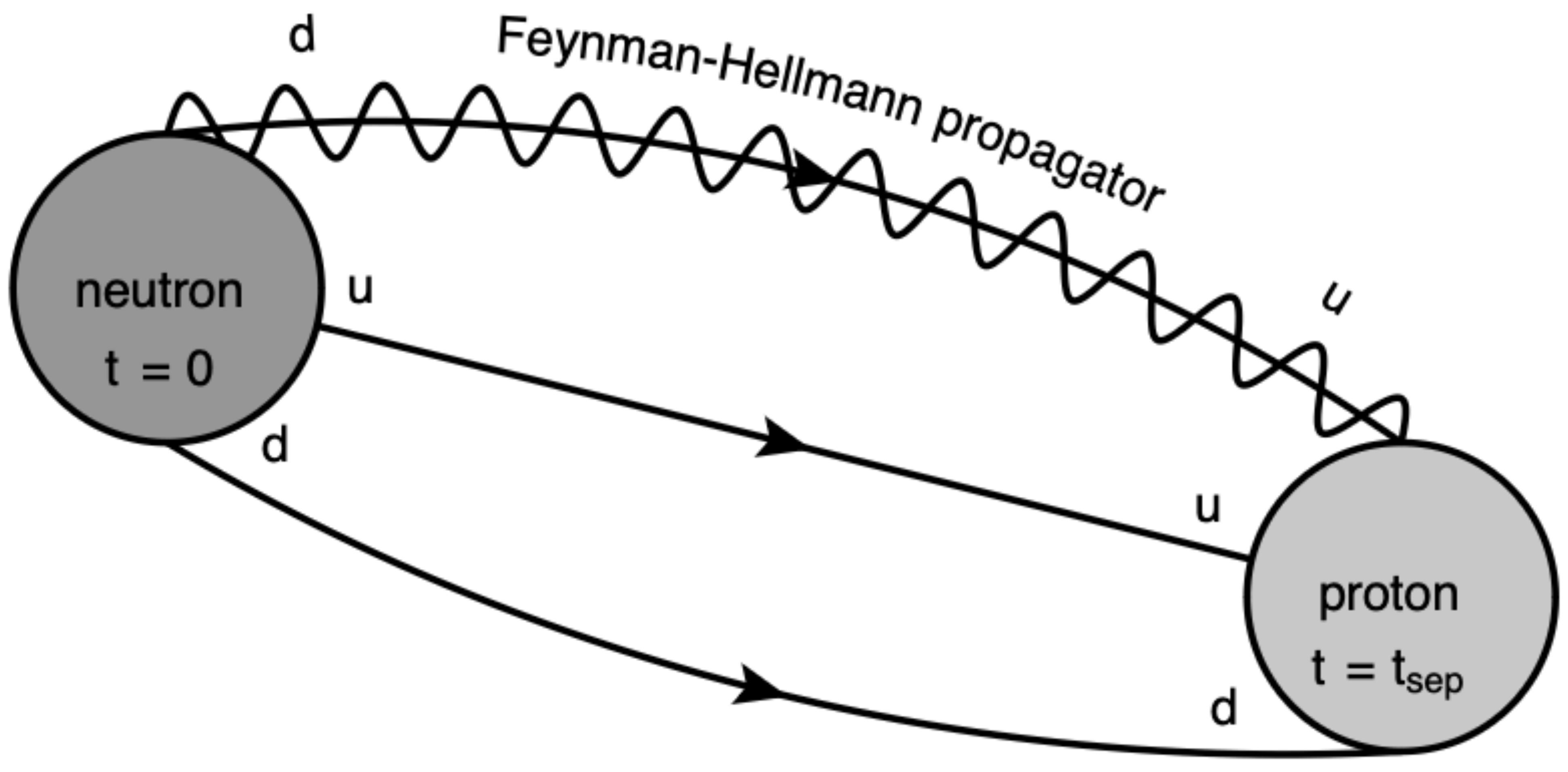

$$-\partial_\lambda C_\lambda(t) = \sum_{n=0}^{N} (t-1)\left[|A_n|^2\, g_{nn}^{\Gamma} - d_n\right] e^{-E_n t} + 2\sum_{n<m} A_n A_m^\dagger\, g_{nm}^{\Gamma}\, e^{(-E_n+\Delta_{mn}/2)t} \times \frac{\sinh\left[\Delta_{mn}(t+1)/2\right]}{\sinh\left(\Delta_{mn}/2\right)}$$

Image credit: Nature 558, 91–94 (2018)

Lattice QCD Ensembles

Parameter Space**

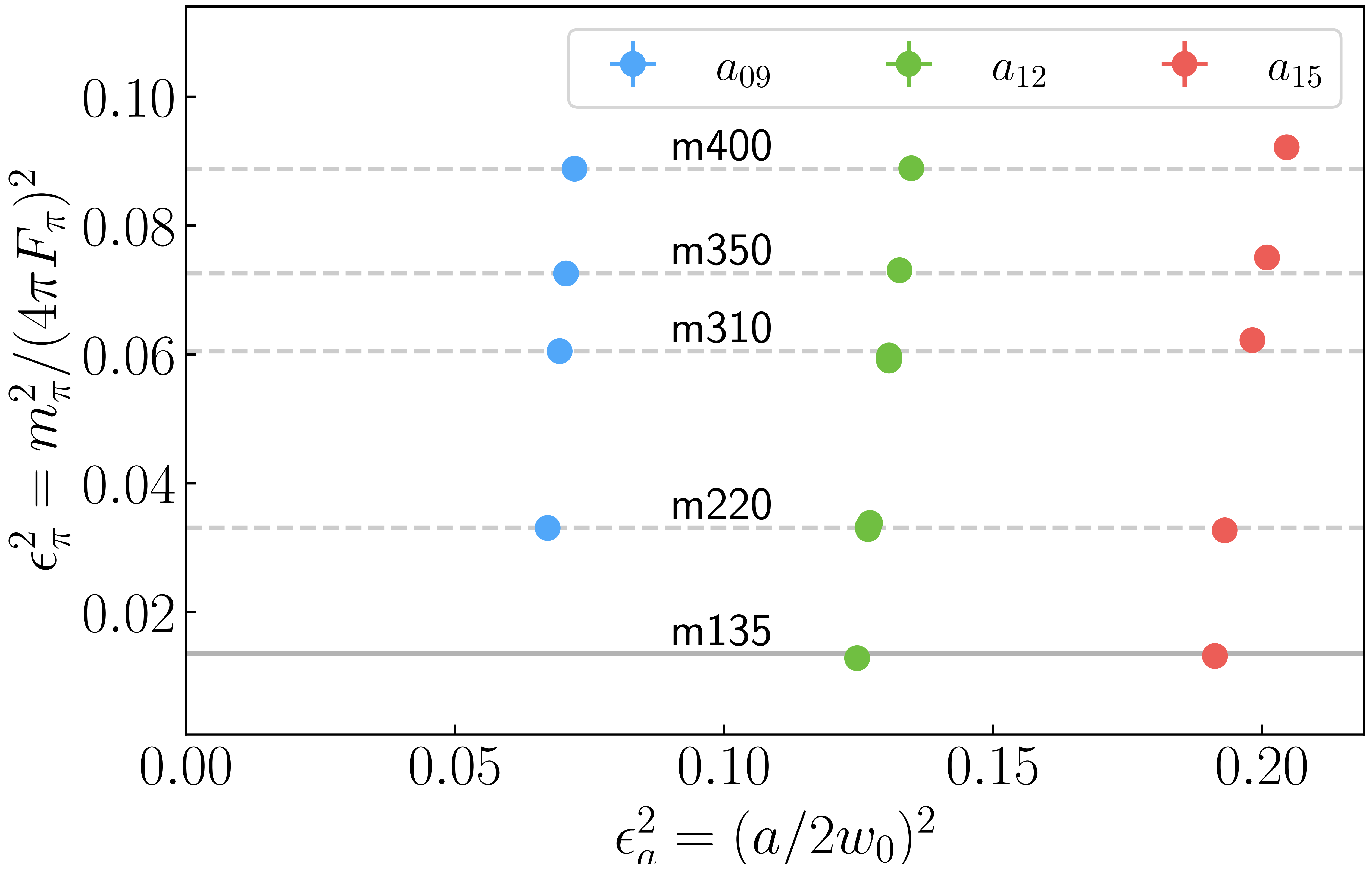

Lattice observables are calculated at several m_π, FV, and finite a

g_A calculated on 18 ensembles

$\epsilon_\pi = \dfrac{m_\pi}{4\pi F_\pi}$

$m_\pi L$

$\epsilon_a = \dfrac{a}{2w_0}$

Need a simultaneous chiral, infinite volume, continuum extrapolation

g_A^{phys}

This work: arXiv: 2503.09891 [hep-lat]

*Mixed-Action: Möbius Domain-wall fermions solved on 2+1+1 gradient flowed HISQ ensembles. A subset of HISQ configurations are provided by the MILC collaboration. **New a15m310L,XL

Numerical Observations from LQCD

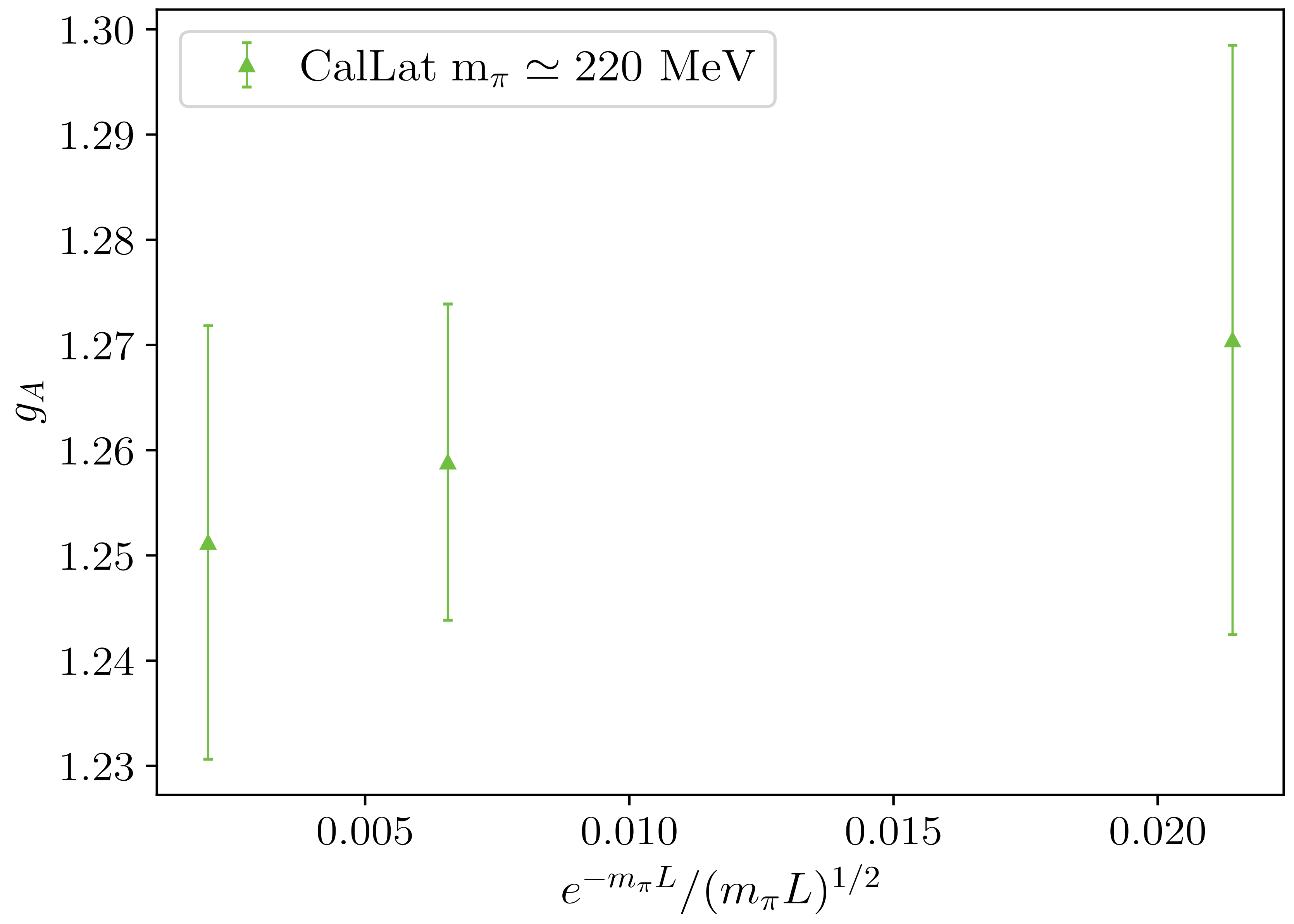

- For nucleon matrix element calculations NLO FV contributions used to describe the entire range of pion masses:

$$\delta_{\mathrm{FV}}^{(2)} = 4\epsilon_\pi^2 g_0 \sum_{\vec{n}\neq 0} \left[\frac{2g_0^2}{3} K_0(m_\pi L|\vec{n}|) - \left(1 + \frac{2g_0^2}{3}\right) \frac{K_1(m_\pi L|\vec{n}|)}{m_\pi L|\vec{n}|} \right]$$

- In the asymptotically large $m_\pi L$ limit:

$$\boxed{\delta_{\mathrm{FV}}^{(2)} \simeq \frac{\mathrm{e}^{-m_\pi L}}{\sqrt{m_\pi L}}}$$

Numerical Observations from LQCD

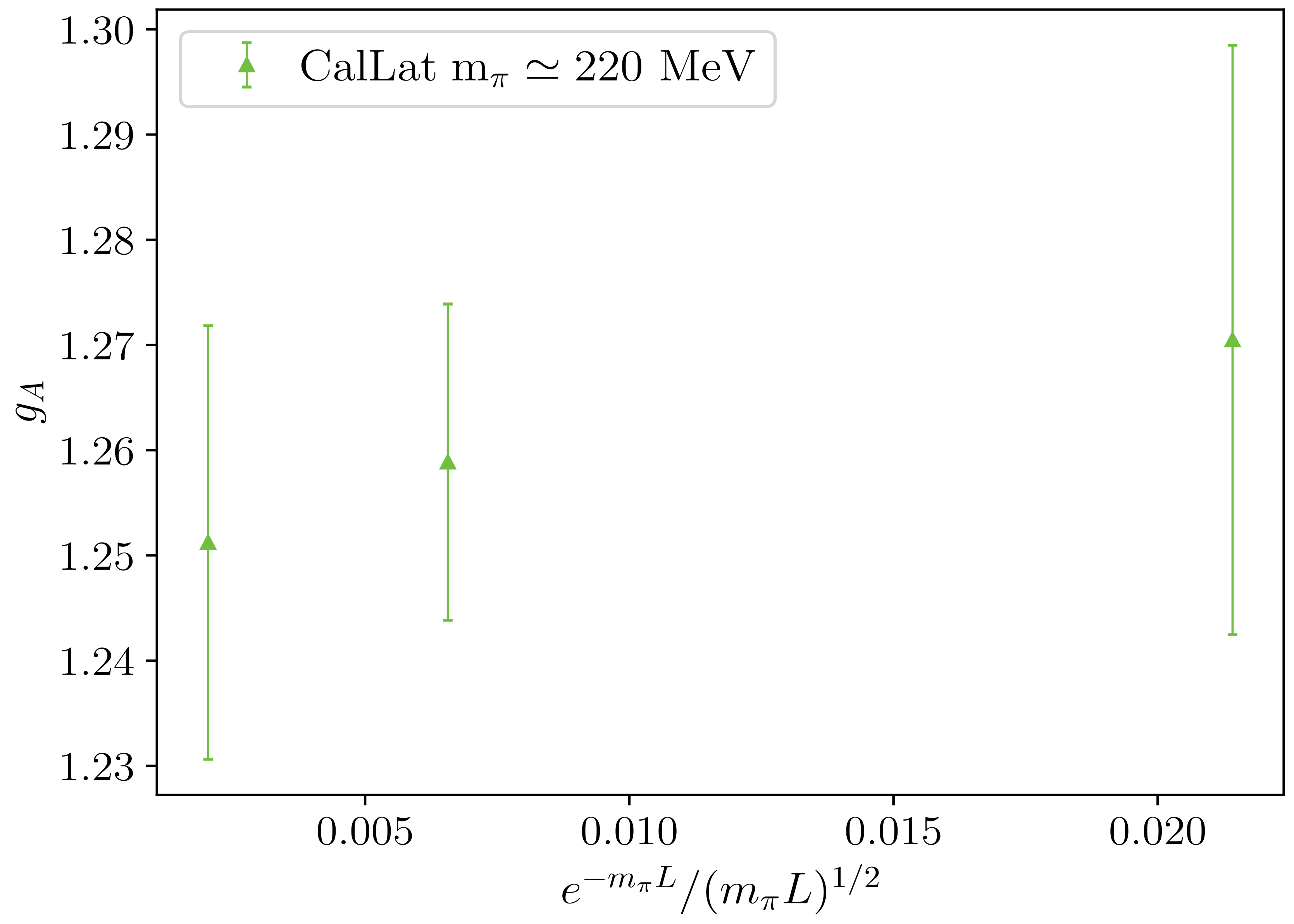

- For nucleon matrix element calculations NLO FV contributions used to describe the entire range of pion masses:

$$\delta_{\rm FV}^{(2)} = 4\epsilon_\pi^2 g_0 \sum_{\vec{n}\neq 0}\left[\frac{2g_0^2}{3}K_0(m_\pi L|\vec{n}|) - \left(1+\frac{2g_0^2}{3}\right)\frac{K_1(m_\pi L|\vec{n}|)}{m_\pi L|\vec{n}|}\right]$$

- Most groups only use the asymptotically large $m_\pi L$ limit:

$$\boxed{\delta_{\rm FV}^{(2)} \simeq c_{\rm v}\frac{e^{-m_\pi L}}{\sqrt{m_\pi L}}}$$

Numerical Observations from LQCD

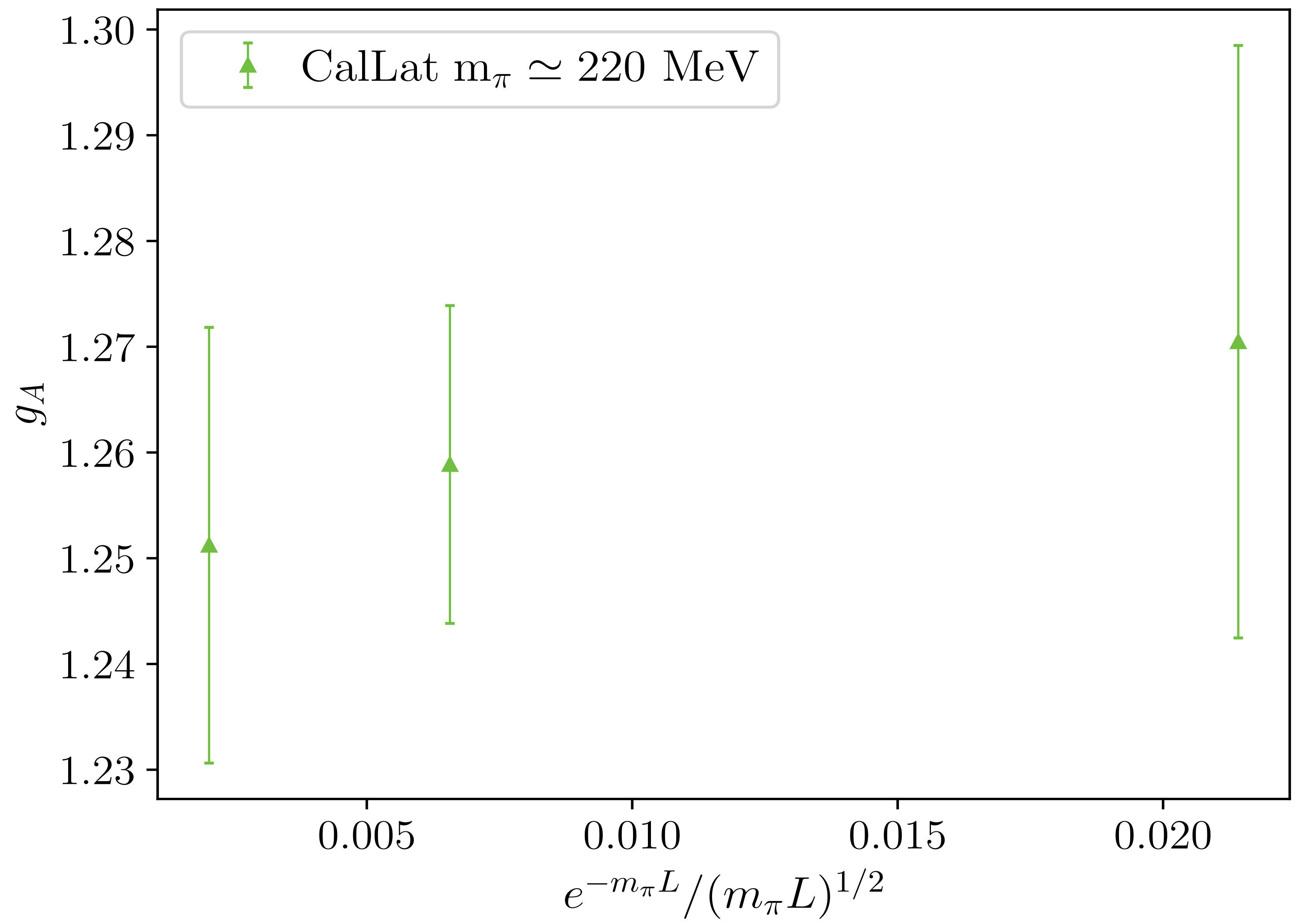

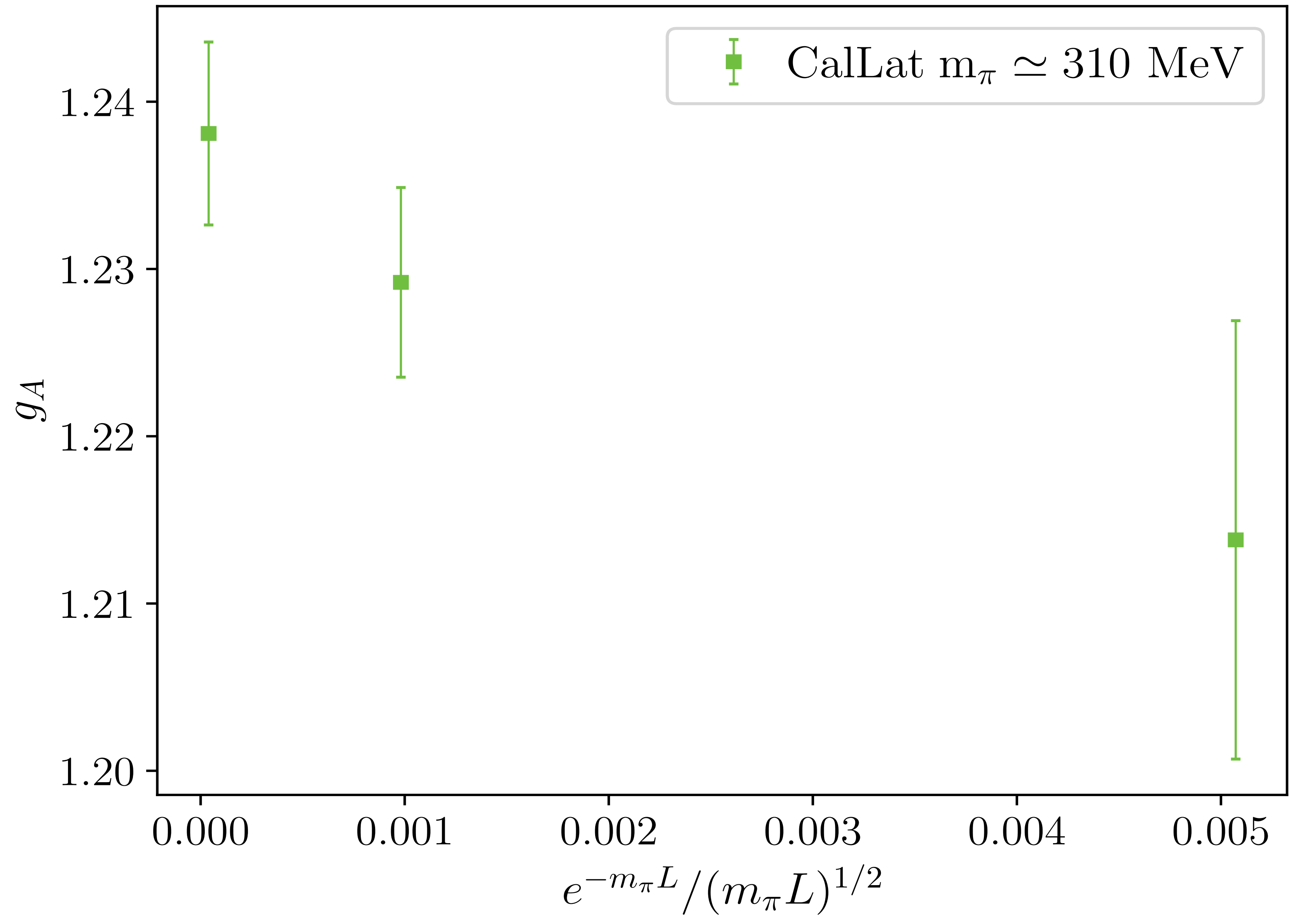

- For nucleon matrix element calculations NLO FV contributions used to describe the entire range of pion masses:

$$\delta_{\rm FV}^{(2)} = 4\epsilon_\pi^2 g_0 \sum_{\vec{n}\neq 0} \left[\frac{2g_0^2}{3} K_0(m_\pi L|\vec{n}|) - \left(1 + \frac{2g_0^2}{3}\right) \frac{K_1(m_\pi L|\vec{n}|)}{m_\pi L|\vec{n}|} \right]$$

- Most groups only use the asymptotically large $m_\pi L$ limit:

$$\boxed{\delta_{\rm FV}^{(2)} \simeq c_{\rm V} \frac{e^{-m_\pi L}}{\sqrt{m_\pi L}}}$$

- CalLat results are consistent SU(2) HBχPT($\not{\Delta}$) at $m_\pi \approx 220$ MeV but the opposite sign at $m_\pi \approx 310$ MeV.

- Do other groups see this behavior?

Beane and Savage PRD 70, 074029 (2004)

Numerical Observations from LQCD

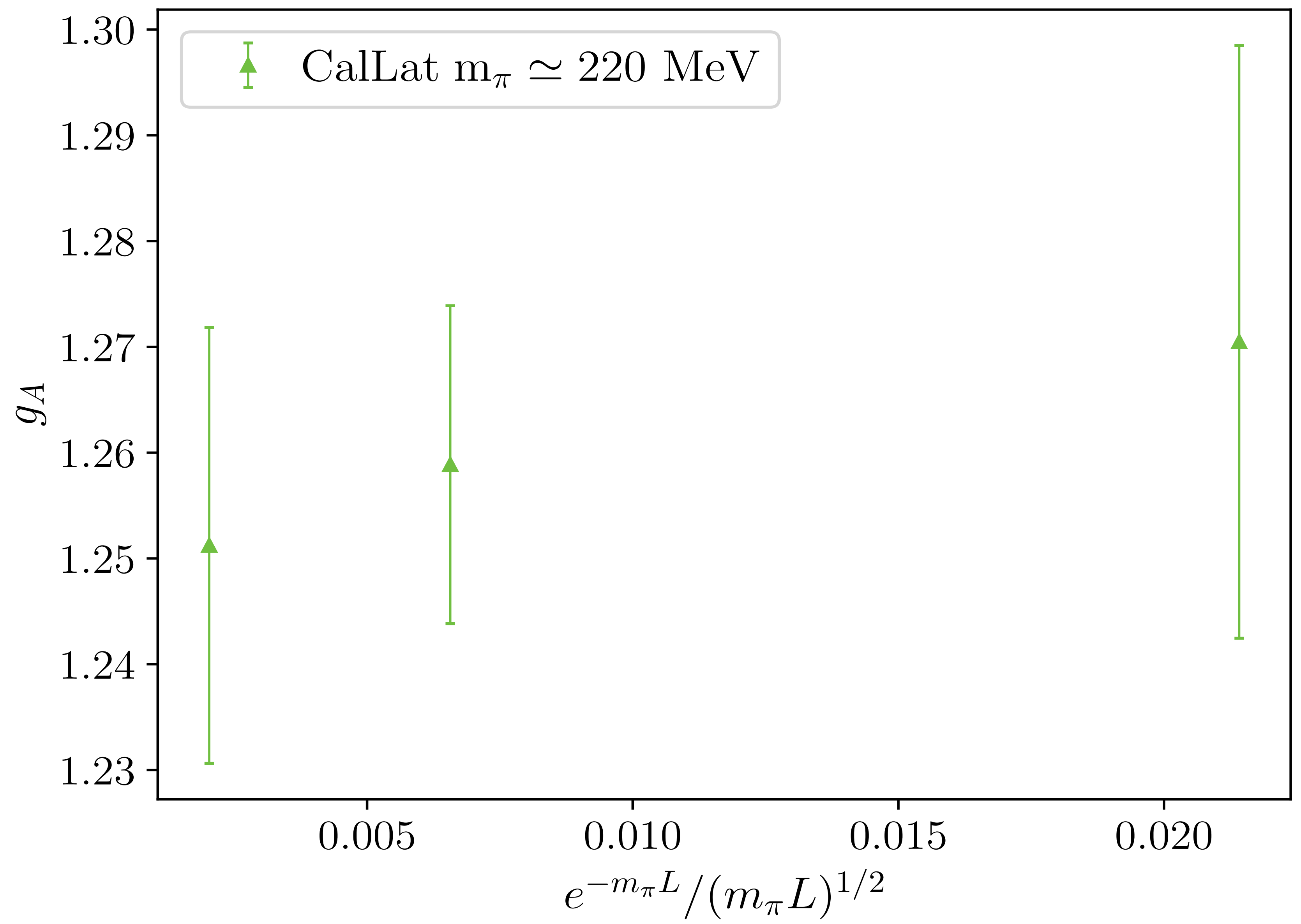

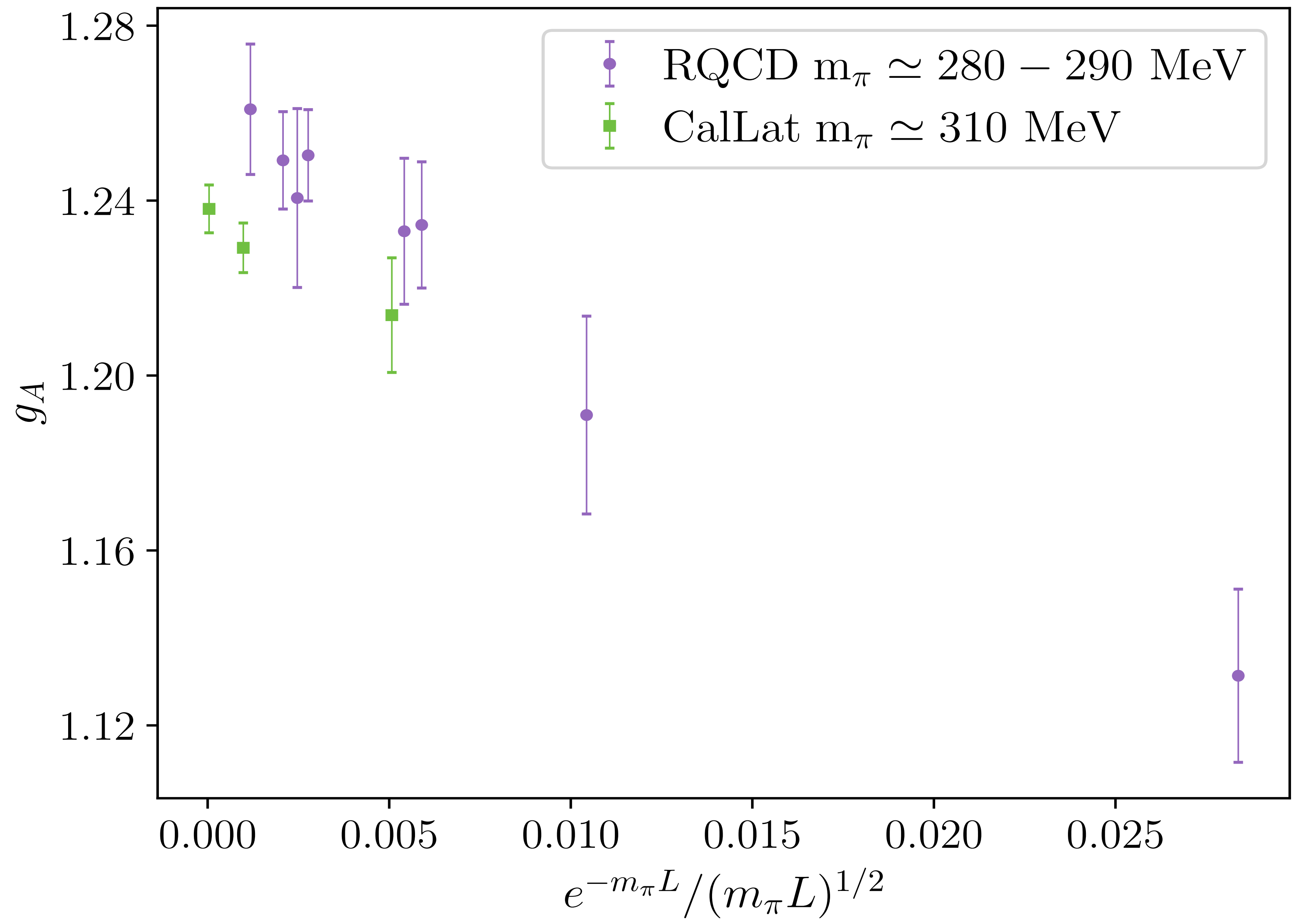

- For nucleon matrix element calculations NLO FV contributions used to describe the entire range of pion masses:

$$\delta_{\mathrm{FV}}^{(2)} = 4\epsilon_\pi^2 g_0 \sum_{\vec{n}\neq 0} \left[\frac{2g_0^2}{3} K_0(m_\pi L|\vec{n}|) - \left(1 + \frac{2g_0^2}{3}\right) \frac{K_1(m_\pi L|\vec{n}|)}{m_\pi L|\vec{n}|} \right]$$

- Most groups only use the asymptotically large $m_\pi L$ limit:

$$\boxed{\delta_{\mathrm{FV}}^{(2)} \simeq c_{\mathrm{V}} \frac{\mathrm{e}^{-m_\pi L}}{\sqrt{m_\pi L}}}$$

- At $m_\pi \approx 285$ MeV the RQCD group shows a statistically significant downward trend.

- Are the NLO FV corrections sufficient to characterize these effects over all m_π? Should one include a model that can change signs at different m_π or $m_\pi L$?

RQCD data: Bali et.al PRD 108, 034512 (2023)
Beane and Savage PRD 70, 074029 (2004)

Extrapolation Analysis

- Taking an agnostic, data-driven approach to determine the model that best represents the data.
- Non-monotonic Pion (Quark) mass and volume dependence parameterized through Chiral Perturbation Theory (χPT) up to $O(\epsilon_\pi^3)$:

$$\epsilon_\pi = \frac{m_\pi}{4\pi F_\pi} \qquad m_\pi L \qquad \epsilon_a = \frac{a}{2w_0}$$

$$g_{A,\chi} = \delta_{\text{FV}}^{(2)} + \delta_{\text{FV}}^{(3)} \qquad g_{A,\chi}^{f_2} = f_2\delta_{\text{FV}}^{(2)} + \delta_{\text{FV}}^{(3)}$$

$$g_{A,\chi}^{f_3} = \delta_{\text{FV}}^{(2)} + f_3\delta_{\text{FV}}^{(3)} \qquad g_{A,\chi}^{f_2,f_3} = f_2\delta_{\text{FV}}^{(2)} + f_3\delta_{\text{FV}}^{(3)}$$

NLO: $$\delta_{\text{FV}}^{(2)} = \frac{8}{3}\epsilon_\pi^2\left[g_0^3 F_1^{(2)}(m_\pi L) + g_0 F_3^{(2)}(m_\pi L)\right]$$

NNLO: $$\delta_{\text{FV}}^{(3)} = \epsilon_\pi^3 g_0 \frac{2\pi}{3}\left\{g_0^2\frac{4\pi F_\pi}{M_N}F_1^{(3)}(m_\pi L) - \left[\frac{4\pi F_\pi}{M_N}(3+2g_0^2) + 4(2\tilde{c}_4 - \tilde{c}_3)\right]F_3^{(3)}(m_\pi L)\right\}$$

- g_0 is the nucleon axial coupling in the chiral limit.

- Monotonic FV models:
  - $g_{A,\text{FV}}^{\text{mono}-1} = f_2\epsilon_\pi^2 F_1^{(2)}$ $\quad g_{A,\text{FV}}^{\text{mono}-2} = f_2\epsilon_\pi^2 F_3^{(2)}$
  - $g_{A,\text{FV}}^{\text{mono}-3} = f_2\epsilon_\pi^2 F_1^{(3)}$ $\quad g_{A,\text{FV}}^{\text{mono}-3} = f_2\epsilon_\pi^2 F_3^{(3)}$

Extrapolation Analysis

- Taking an agnostic, data-driven approach to determine the model that best represents the data.
- Non-monotonic Pion (Quark) mass and volume dependence parameterized through Chiral Perturbation Theory (χPT) up to $O(\epsilon_\pi^3)$:

$$\epsilon_\pi = \frac{m_\pi}{4\pi F_\pi} \qquad m_\pi L \qquad \epsilon_a = \frac{a}{2w_0}$$

$$g_{A,\chi} = \delta_{\rm FV}^{(2)} + \delta_{\rm FV}^{(3)} \qquad g_{A,\chi}^{f_2} = f_2\delta_{\rm FV}^{(2)} + \delta_{\rm FV}^{(3)}$$

$$g_{A,\chi}^{f_3} = \delta_{\rm FV}^{(2)} + f_3\delta_{\rm FV}^{(3)} \qquad g_{A,\chi}^{f_2,f_3} = f_2\delta_{\rm FV}^{(2)} + f_3\delta_{\rm FV}^{(3)}$$

NLO: $\delta_{\rm FV}^{(2)} = \frac{8}{3}\epsilon_\pi^2\left[g_0^3 F_1^{(2)}(m_\pi L) + g_0 F_3^{(2)}(m_\pi L)\right]$

NNLO: $\delta_{\rm FV}^{(3)} = \epsilon_\pi^3 g_0 \frac{2\pi}{3}\left\{g_0^2 \frac{4\pi F_\pi}{M_N} F_1^{(3)}(m_\pi L) - \left[\frac{4\pi F_\pi}{M_N}(3 + 2g_0^2) + 4(2\tilde{c}_4 - \tilde{c}_3)\right] F_3^{(3)}(m_\pi L)\right\}$

- g_0 is the nucleon axial coupling in the chiral limit.

- Monotonic FV models:
  - $g_{A,\rm FV}^{\rm mono-1} = f_2\epsilon_\pi^2 F_1^{(2)}$ $\quad g_{A,\rm FV}^{\rm mono-2} = f_2\epsilon_\pi^2 F_3^{(2)}$
  - $g_{A,\rm FV}^{\rm mono-3} = f_2\epsilon_\pi^2 F_1^{(3)}$ $\quad g_{A,\rm FV}^{\rm mono-3} = f_2\epsilon_\pi^2 F_3^{(3)}$
- Discretization models:
  - $g_{A,a}^{(2)} = a_2\epsilon_a^2$
  - $g_{A,a}^{(4)} = a_2\epsilon_a^2 + b_4\epsilon_a^2\epsilon_\pi^2 + a_4\epsilon_a^4$

Extrapolation Analysis

- Taking an agnostic, data-driven approach to determine the model that best represents the data.
- Non-monotonic Pion (Quark) mass and volume dependence parameterized through Chiral Perturbation Theory (χPT) up to $O(\epsilon_\pi^3)$:

$$\epsilon_\pi = \frac{m_\pi}{4\pi F_\pi} \qquad m_\pi L \qquad \epsilon_a = \frac{a}{2w_0}$$

$$g_{A,\chi} = \delta_{\mathrm{FV}}^{(2)} + \delta_{\mathrm{FV}}^{(3)} \qquad g_{A,\chi}^{f_2} = f_2\delta_{\mathrm{FV}}^{(2)} + \delta_{\mathrm{FV}}^{(3)}$$

$$g_{A,\chi}^{f_3} = \delta_{\mathrm{FV}}^{(2)} + f_3\delta_{\mathrm{FV}}^{(3)} \qquad g_{A,\chi}^{f_2,f_3} = f_2\delta_{\mathrm{FV}}^{(2)} + f_3\delta_{\mathrm{FV}}^{(3)}$$

NLO: $\delta_{\mathrm{FV}}^{(2)} = \frac{8}{3}\epsilon_\pi^2\left[g_0^3F_1^{(2)}(m_\pi L) + g_0F_3^{(2)}(m_\pi L)\right]$

NNLO: $\delta_{\mathrm{FV}}^{(3)} = \epsilon_\pi^3 g_0\frac{2\pi}{3}\left\{g_0^2\frac{4\pi F_\pi}{M_N}F_1^{(3)}(m_\pi L) - \left[\frac{4\pi F_\pi}{M_N}(3+2g_0^2) + 4(2\tilde{c}_4 - \tilde{c}_3)\right]F_3^{(3)}(m_\pi L)\right\}$

- g_0 is the nucleon axial coupling in the chiral limit.

- Monotonic FV models:
  - $g_{A,\mathrm{FV}}^{\mathrm{mono}-1} = f_2\epsilon_\pi^2 F_1^{(2)}$ $\quad g_{A,\mathrm{FV}}^{\mathrm{mono}-2} = f_2\epsilon_\pi^2 F_3^{(2)}$
  - $g_{A,\mathrm{FV}}^{\mathrm{mono}-3} = f_2\epsilon_\pi^2 F_1^{(3)}$ $\quad g_{A,\mathrm{FV}}^{\mathrm{mono}-3} = f_2\epsilon_\pi^2 F_3^{(3)}$
- Discretization models:
  - $g_{A,a}^{(2)} = a_2\epsilon_a^2$
  - $g_{A,a}^{(4)} = a_2\epsilon_a^2 + b_4\epsilon_a^2\epsilon_\pi^2 + a_4\epsilon_a^4$

This work: arXiv: 2503.09891 [hep-lat]

LECs and Convergence

- c_3 and c_4 have been determined from pheno N^{3}LO analysis of πN scattering data -> large combination.
- Yet our determination from this g_A analysis gives a result 20 times smaller. -> Insensitive to large prior widths.
- While this is extreme, the literature shows these values are hard to pin down from πN scattering.

$$g_{A,\chi} = g_0 + \delta_\chi^{(2)} + \delta_\chi^{(3)}$$

NLO: $$\delta_\chi^{(2)} = \epsilon_\pi^2\left[-(g_0+2g_0^3)\ln\epsilon_\pi^2 + \tilde{d}_{16} - g_0^3\right]$$

NNLO: $$\delta_\chi^{(3)} = \epsilon_\pi^3 g_0 \frac{2\pi}{3}\left[3(1+g_0^2)\frac{4\pi F_\pi}{M_N} + 4(2\tilde{c}_4 - \tilde{c}_3)\right]$$

$$\begin{aligned} c_3 &= -5.61(6)\ \mathrm{GeV}^{-1} \\ c_4 &= \ \ 4.26(4)\ \mathrm{GeV}^{-1} \\ 2c_4 - c_3 &= \ \ 14.1(1)\ \mathrm{GeV}^{-1} \end{aligned}$$

Phenomenology

$$2c_4 - c_3 = (0.66\text{–}0.70)\ \mathrm{GeV}^{-1}$$

LQCD

$\delta_\chi^{(n)}(\epsilon_\pi^{\mathrm{phys}})$	g_0	$\delta_\chi^{(2)}$	$\delta_\chi^{(3)}$
	1.226(15)	−0.007(11)	0.0507(53)

source	g_0	$g_0(1+2g_0^2)$	$4\tilde{d}_{16}^r - g_0^3$	$\delta_\chi^{(3)}/\epsilon_\pi^3$
Phenomenology	1.2(1)	4.7(1.0)	–	187(18)
LQCD analysis	1.22(2)	4.9(0.2)	−21(2)	32(3)

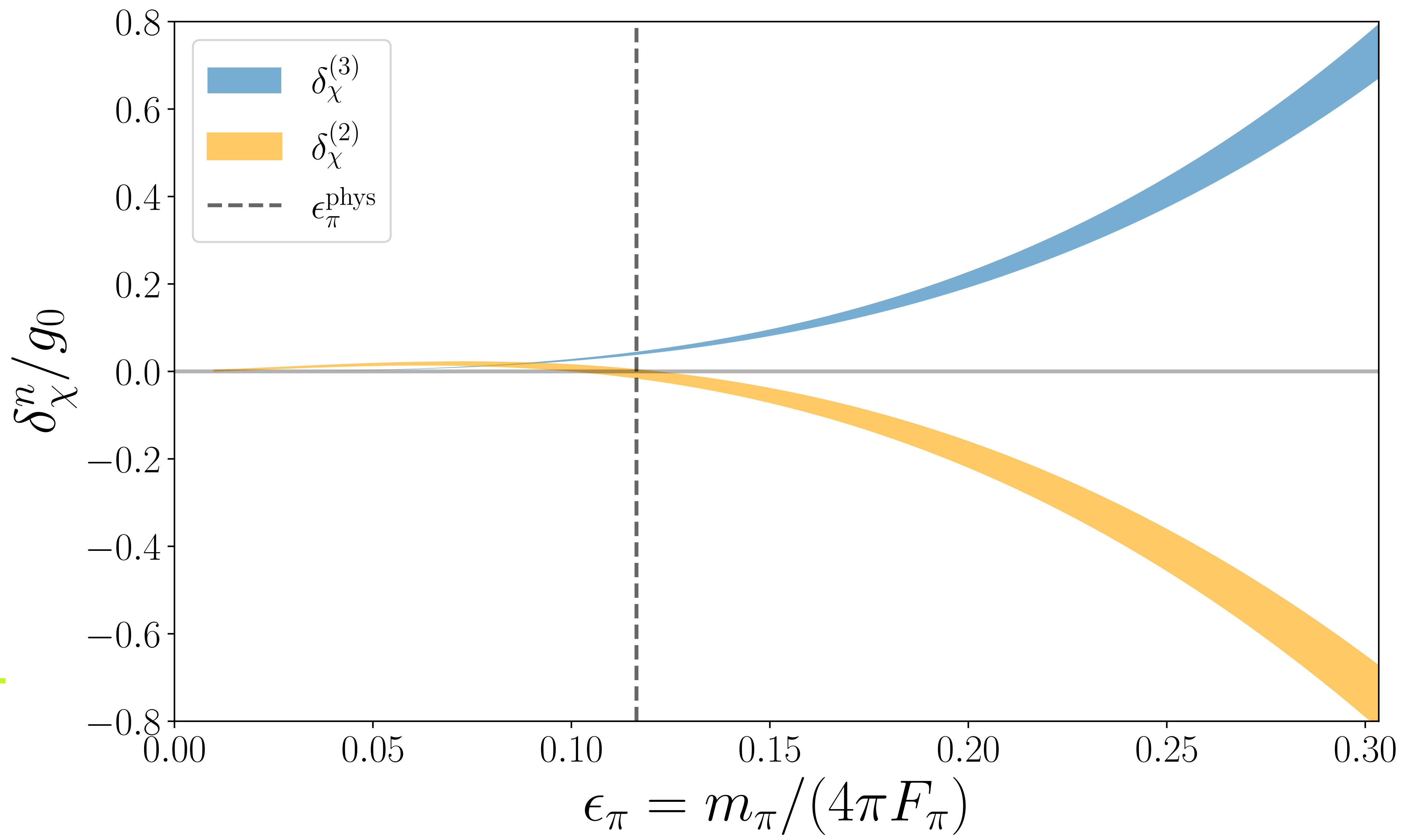

- For $\epsilon_\pi \geq \epsilon_\pi^{\mathrm{phys}}$, $\delta_\chi^{(2)}$ and $\delta_\chi^{(3)}$ have opposite signs and seem relatively comparable in size.
- Near cancellation between terms at $\delta_\chi^{(2)}$
- Very large refactor for $\delta_\chi^{(3)}$, but improved with LQCD.

Expectations from χPT and Large-N_c

- The chiral expansion for nucleons is a series in $\epsilon_\pi = \dfrac{m_\pi}{4\pi F_\pi}$, while for pions, it is in ϵ_π^2.
  - Higher-order contributions are relatively more important.
- The nucleon has a richer spectrum of excited states ($N\pi$, $\Delta\pi, \ldots$)
- For both IV and FV, there is already a discrepancy that arises at *NLO* when comparing constraints from large-N_c on g_A^{Δ} and $g_A^{(\cancel{\Delta})}$.

$$g_A^{(\cancel{\Delta})} = g_0 + \epsilon_\pi^2\left[-(g_0 + 2g_0^3)\ln\epsilon_\pi^2 + \tilde{\mathrm{d}}_{16} - \mathrm{g}_0^3\right]$$

$$\begin{aligned}
g_A^{(\Delta)} = {} & g_0\left[1 - \epsilon_\pi^2\ln\epsilon_\pi^2\right] + \epsilon_\pi^2(4\tilde{d}_{16}^{r,\Delta} - g_0^3) \\
& -2\epsilon_\pi^2\ln\epsilon_\pi^2\left[\mathrm{g}_0^3 + \frac{1}{9}\mathrm{g}_0\mathrm{g}_{\mathrm{N}\Delta}^2 + \frac{25}{81}\mathrm{g}_\Delta\mathrm{g}_{\mathrm{N}\Delta}^2\right] \\
& -R\left(\frac{m_\pi^2}{\Delta^2}\right)g_{N\Delta}^2\left[\epsilon_\pi^2\frac{32}{27}g_0 + \epsilon_\Delta^2\left(\frac{76}{27}g_0 + \frac{100}{81}g_\Delta\right)\right] \\
& +\frac{32}{27}g_0 g_{N\Delta}^2\epsilon_\pi^2\left[1 + \ln\frac{4\epsilon_\Delta^2}{\epsilon_\pi^2} + \frac{\pi\epsilon_\pi}{\epsilon_\Delta}\right] \\
& +\frac{2}{81}g_{N\Delta}^2\epsilon_\pi^2\left(9g_0 + 25g_\Delta\right)\left[1 + \ln(4\epsilon_\Delta^2)\right]
\end{aligned}$$

$$\Delta = m_\Delta - m_N$$

$$\epsilon_\Delta = \frac{\Delta}{4\pi F_\pi}$$

Expectations from χPT and Large-N_c

- The chiral expansion for nucleons is a series in $\epsilon_\pi = \dfrac{m_\pi}{4\pi F_\pi}$, while for pions, it is in ϵ_π^2.
  - Higher-order contributions are relatively more important.
- The nucleon has a richer spectrum of excited states ($N\pi$, $\Delta\pi, \ldots$)
- For both IV and FV, there is already a discrepancy that arises at *NLO* when comparing constraints from large-N_c on g_A^{Δ} and $g_A^{(\not\Delta)}$.
- Ultimately, there is an ambiguity of the sign of *NLO FV* corrections depending on the parameters and constraints.

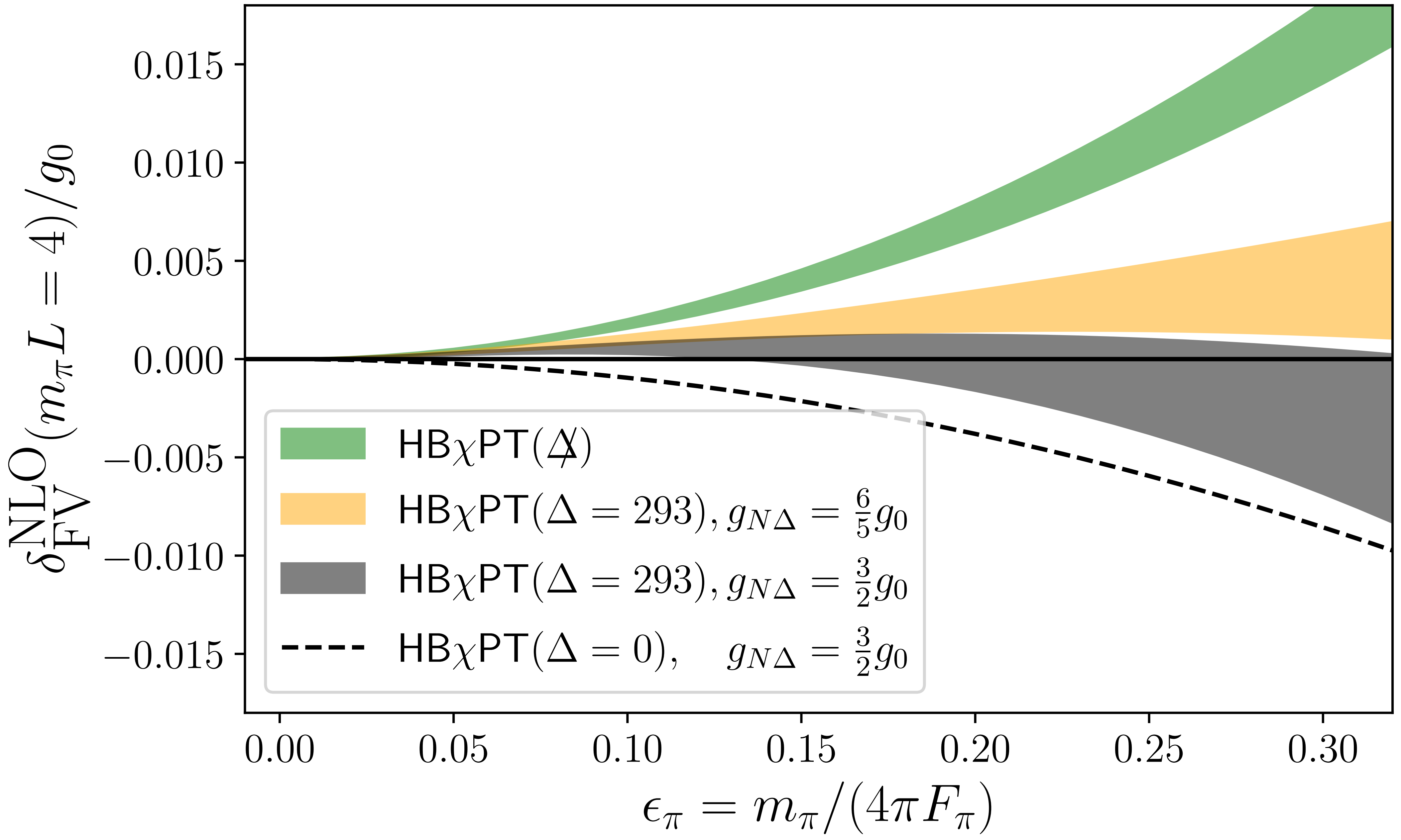

- If one wishes to include the possibility of non-monotonic FV corrections, g_A^{Δ} up to *NLO* is need or $g_A^{(\not\Delta)}$ up to *NNLO*.